

Electronic Supplementary Material

Triphenylamine-functionalized aza-BODIPY dyes: synthesis, characterization, and their application as hole transport materials in perovskite solar cells

Junjun Su,^a Li Zhu,^a Zixuan Dong,^a Mengqi Liu,^a Fei Zhang,^{a,b} Xianggao Li,^{a,b}
Shirong Wang,^{*a,b} and Zhijian Chen^{*a,b}

^a *Tianjin University, School of Chemical Engineering and Technology, Tianjin
300072, China.*

^b *School of Chemical Engineering and Technology, Collaborative Innovation Center
of Chemical Science and Chemical Engineering (Tianjin), Tianjin University, Tianjin*

*E-mail: wangshirong@tju.edu.cn

*E-mail: zjchen@tju.edu.cn

Table of Contents

1. Materials and methods	S3
2. Synthesis and characterization of the aza-BODIPY dyes	S7
3. Perovskite solar cell fabrication and characterization	S49
4. References.....	S55

1. Materials and methods

Materials: All materials, solvents and reagents were purchased from commercial suppliers and used without further purification, unless otherwise noted. Silica gel (300-400 mesh) was used for columnar chromatography. FAI (>99.95%) and MABr (>99.95%) were purchased from Luminescence Technology Corporation. PbI₂ (≥99.99%), PbBr₂ (≥99.99%), CsI (≥99.99%), were obtained from Xi'an Polymer Light Technology Corp. Fluorine-doped tin-oxide-coated glass (7 Ω per square) was purchased from Yingkou Advanced Election Technology Co., Ltd. TiO₂ paste (30 NR-D, >99.9%) was purchased from Dyesol. Titanium diisopropoxide bis(acetylacetonate) (75wt.% in isopropanol), acetylacetone (≥99.5%), anhydrous dimethyl sulfoxide (DMSO, 99.8%), *N,N'*-dimethylformamide (DMF, 99.8%) and chlorobenzene (99.9%) were purchased from Aladdin.

General Methods

Chemicals and reagents: Solvents and reagents purchased from commercial suppliers were used without further purification, unless otherwise stated. Anhydrous dichloromethane (DCM) was distilled over CaH₂. Products were purified by column chromatography with silica gel (300-400 mesh).

NMR spectroscopy: The ¹H and ¹³C NMR spectra of the compounds were recorded on Bruker AVANCE III HD (400 MHz) spectrometer with tetramethylsilane (TMS) as internal standard at room temperature. The multiplicities of proton signals are abbreviated as *s*, *d*, *t*, and *m* respectively, indicating singlet, doublet, triplet, and multiplet.

Mass spectra: High resolution mass spectra (ESI) were measured on a Bruker micro TOF-QII mass spectrometer. Other mass spectrometry analyses were measured using a Bruker Autoflex III MALDI-TOF instrument.

UV/Vis absorption spectroscopy: UV/Vis absorption spectra were recorded on an Agilent Technologies Cary 300 UV/Vis spectrophotometer equipped with a SPV 1 × 1 temperature controller. The solvents for spectroscopic studies were spectroscopic grade.

The spectra were recorded in quartz glass cuvettes and the molar extinction coefficients ϵ was calculated according to Lambert-Beer's law: $A = \epsilon cl$.

Fluorescence Spectroscopy. The steady-state (PL) and time-resolved fluorescence (TRPL) spectra were measured using an Edinburgh FLS1000 spectrofluorometer, and all the fluorescence spectra were corrected. The TRPL measurements were conducted with a picosecond pulsed diode laser emitting at a wavelength of 475 nm. The photoluminescence decay behavior of pure perovskite on FTO glass/ Al_2O_3 was characterized by a single exponential function. After depositing these HTMs on the perovskite making them into devices composed of FTO glass/ Al_2O_3 /perovskite/HTM structures. The TRPL spectra of perovskite coated with **1-3** on FTO glass/ Al_2O_3 show a bi-exponential trend. The time-resolved spectrum of the dye solution was measured using. The pulsed light emitting diode laser (560 nm / 680 nm, 10 MHz) was used as the excitation source. A (Hamamatsu R3809) micro channel plate photomultiplier was used as detector. The instrument response was collected by scattering the exciting light of a dilute, aqueous suspension of colloidal silica (Ludox). Decay curves were evaluated using the software supplied with the instrument applying least square regression analysis. The quality of the fit was evaluated by analysis of χ^2 (0.9-1.1), as well as by inspection of residuals and autocorrelation function.

Atomic Force Microscope (AFM) measurements: AFM measurements were performed on perovskite thin films coated with dye under ambient conditions using a Bruker Dimension Icon atomic force microscope.

Thermogravimetric analysis (TGA): TGA was measured by TGA Q50 thermogravimetric apparatus in heating rate of $20\text{ }^\circ\text{C}\cdot\text{min}^{-1}$.

Melting Point Determination: The melting point of the synthesized compound was determined using a hot-stage microscope (Model: CKX53, Olympus Corporation, Japan). A small amount of the sample was placed on the stage, and the temperature was gradually increased at a controlled rate. The sample was carefully observed under the microscope to detect the point at which the solid phase transitioned into a liquid. The temperature at which complete melting occurred was recorded as the melting point of the compound.

Hole Mobility Measurements. Hole mobilities of different HTMs were measured by using the space-charge-limited-current (SCLC) method¹ with a device configuration of ITO/PEDOT/HTMs/Au. In the process of devices fabrication, ITO substrates were first cleaned with O₂ plasma treatment for 10 min. Then PEDOT:PSS was spin-coated on ITO substrates at 4000 rpm for 30 s and followed by annealing step at 130 °C for 30 min. The thickness (*D*₁) of PEDOT:PSS was measured using the surface profile method and recorded with a KLA-Tencor Alpha-Step D300. The aza-BODIPY **1-3** solution with a concentration of 20 mg mL⁻¹ was spin-coated at speeds of 2000 rpm s⁻¹, 3000 rpm s⁻¹ and 1500 rpm s⁻¹ for a duration of 30 s. The thicknesses (*D*₂) of the HTM and PEDOT:PSS films were measured. The thicknesses (*D*) of the HTM films were obtained by $D = D_1 - D_2$. Finally, a 100 nm thick Au layer was deposited under high vacuum. The current density-voltage (*J-V*) curves were measured using Keithley 2000 and Keithley 2400 digital source meter. Hole mobilities were calculated using the Mott-Gurney Law (1):

$$J = \frac{9\mu\epsilon_0\epsilon_r V^2}{8D^3} \quad (1)$$

Here, *J* was the current density, μ was the hole mobility, ϵ_0 was the vacuum permittivity of the free space ($8.85 \times 10^{-12} \text{ F}\cdot\text{m}^{-1}$), ϵ_r was the average dielectric constant of the HTMs (≈ 3). *V* was the applied bias, and *D* (aza-BODIPY **1**, 137 nm; aza-BODIPY **2**, 126 nm; aza-BODIPY **3**, 151 nm) was the thickness of the HTL films.

Cyclic voltammetry curve: In the experiment, the platinum disk electrode was used as the working electrode, the platinum wire was used as the pair electrode, and the silver wire was used as the pseudo reference electrode. The solvent was dried methylene chloride at a concentration of $1.0 \times 10^{-4} \text{ M}$. The electrolyte was tetrabutylammonium hexafluorophosphate, the electrolyte concentration was 0.1 M, and the scanning rate was $50 \text{ mV}\cdot\text{s}^{-1}$. The internal standard is ferrocene with an energy level of -4.78 eV (relative to the vacuum level) of Fc/Fc⁺.

Single-crystal structure: The crystals were prepared using the solvent diffusion method, with dichloromethane as the good solvent and n-hexane as the poor solvent. A

suitable crystal was selected and on a Rigaku mm007 Saturn 944+ diffractometer. The crystal was kept at 113.15 K during data collection. Using Olex2², the structure was solved with the SHELXT³ structure solution program using Intrinsic Phasing and refined with the SHELXL⁴ refinement package using Least Squares minimisation.

2. Synthesis and characterization of the aza-BODIPY dyes

(E)-3-(4-(diphenylamino)phenyl)-1-phenylprop-2-en-1-one (Compound 4): 1-(4-(Diphenylamino))benzaldehyde (2.18 g, 7.98 mmol, 1.0 eq) was dissolved in 50 mL ethanol in a 250 mL two-necked flask, and 7 mL K₂CO₃ solution (2.5 M) was added to the solution through a dropping funnel. Then acetophenone (0.958 g, 7.98 mmol, 1.0 eq) dissolved in ethanol (20 mL) was slowly added dropwise to the reaction system and stirred at room temperature for 24 h. The reaction mixture was filtered and the filter cake was washed with water until the filtrate became neutral. Then the residue was recrystallized with CH₂Cl₂ and *n*-hexane to give an orange solid (2.60 g, yield: 89.8%); ¹H NMR (400 MHz, CDCl₃, ppm): δ = 7.82 (d, *J* = 8.7 Hz, 2H), 7.71 (d, *J* = 15.7 Hz, 1H), 7.52 (s, 2H), 7.44 (d, *J* = 15.6 Hz, 1H), 7.29 (s, 3H), 7.21 (d, *J* = 7.9 Hz, 3H), 7.10-7.00 (m, 6H), 6.94 (d, *J* = 8.7 Hz, 3H) ppm; ¹³C NMR (101 MHz, CDCl₃, ppm): δ = 189.55, 149.15, 145.78, 143.69, 137.60, 131.45, 128.71, 128.48, 127.52, 127.37, 126.77, 124.45, 123.10, 120.52, 118.36; HRMS (ESI): calculated for C₂₇H₂₁NO [M+H]⁺ = 376.1623 *m/z*, found 376.1623 *m/z*.

(E)-1-(4-(diphenylamino)phenyl)-3-phenylprop-2-en-1-one (Compound 5): 1-(4-(Diphenylamino))acetophenone (2.27 g, 7.98 mmol, 1.0 eq) was dissolved in 50 mL of ethanol in a 250 mL two-necked flask. and 7 mL K₂CO₃ solution (2.5 M) was added to the solution through a dropping funnel. Then, benzaldehyde (0.837 g, 7.98 mmol, 1.0 eq) in ethanol (20ml) was slowly added dropwise to the reaction system and stirred at room temperature for 24 h. The reaction mixture was filtered and the filter cake was washed with water until the filtrate became neutral, then the residue was recrystallized with CH₂Cl₂ and *n*-hexane to give an orange-yellow solid (2.60 g, yield: 89.8%); ¹H NMR (400 MHz, CDCl₃, ppm): δ = 7.84 (d, *J* = 8.7 Hz, 2H), 7.73 (d, *J* = 15.7 Hz, 1H), 7.58-7.43 (m, 3H), 7.31 (s, 3H), 7.23 (d, *J* = 7.9 Hz, 4H), 7.07 (dd, *J* = 15.5, 7.2 Hz, 6H), 6.96 (d, *J* = 8.7 Hz, 2H); ¹³C NMR (101 MHz, CDCl₃, ppm): δ = 187.13, 151.05, 145.40, 142.51, 134.13, 129.50, 129.18, 129.12, 128.57, 127.85, 127.28, 124.93, 123.63, 120.83, 118.76; HRMS (ESI): calculated for C₂₇H₂₁NO [M+H]⁺ = 376.1623 *m/z*, found 376.1623 *m/z*.

(E)-1,3-bis(4-(diphenylamino)phenyl)prop-2-en-1-one (Compound 6): 1-(4-(Diphenylamino))acetophenone (1.25 g, 4.40 mmol, 1.0 eq) and 1-(4-(diphenylamino))benzaldehyde (1.2 g, 4.40 mmol, 1.0 eq) were dissolved in CH₂Cl₂ (100 mL) in a 250 mL single-necked flask. The solvent was removed by rotary evaporation to obtain a uniform mixture of 1-(4-(diphenylamino))acetophenone and 1-(4-(diphenylamino))benzaldehyde. The mixture and ethanol(70 mL) were added to a 250 mL two-neck flask. 7 mL KOH solution (2M) was added to the system through a dropping funnel and then the solution was stirred at 50 °C for 24 h. After the reaction was completed, the reaction system was cooled to room temperature. The reaction mixture was filtered and the filter cake was washed with water until the filtrate became neutral, then the residue was recrystallized with CH₂Cl₂ and *n*-hexane to give an orange-red solid (2.15 g, yield: 90.0%); ¹H NMR (400 MHz, CDCl₃, ppm): δ = 7.90 (d, *J* = 8.9 Hz, 2H), 7.76 (d, *J* = 15.5 Hz, 1H), 7.48 (d, *J* = 8.7 Hz, 2H), 7.40 (d, *J* = 15.5 Hz, 1H), 7.36-7.26 (m, 8H), 7.21-7.06 (m, 12H), 7.03 (dd, *J* = 8.7, 3.8 Hz, 4H); ¹³C NMR (101 MHz, CDCl₃, ppm): δ = 188.28, 151.90, 149.91, 146.94, 146.60, 143.44, 131.11, 130.03, 129.62, 129.59, 129.51, 128.29, 125.93, 125.40, 124.57, 124.02, 121.79, 120.03, 119.30; MS (MALDI-TOF): calculated for C₃₉H₃₀N₂O [M]⁺ = 542.2358 *m/z*, found 542.2359 *m/z*.

3-(4-(diphenylamino) phenyl)-4-nitro-1-phenylbutan-1-one (Compound 7): Compound 4 (1.67 g, 4.53 mmol, 1.0 eq), nitromethane (1.38 g, 22.66 mmol, 5.0 eq), and diethylamine (1.68 g, 22.68 mmol, 5.0 eq) were dissolved in ethanol (150 mL) and then the solution was refluxed in a 250 mL two-necked flask for 12 h and the progress was monitored by TLC. After the reaction was completed, the reaction system was cooled to room temperature and the solvent was removed by rotary evaporation. The product was dissolved in ethyl acetate (30 mL), then washed with water (50 mL × 3). The organic layer was washed with brine and dried with anhydrous magnesium sulfate. After removing the solvents by evaporation, the residue was separated by column chromatography (petroleum ether:CH₂Cl₂ = 1:1) to afford an orange solid (1.42 g, 72%); ¹H NMR (400 MHz, CDCl₃, ppm): δ = 7.85 (d, *J* = 7.4 Hz, 2H), 7.51 (t, *J* = 7.4 Hz,

1H), 7.39 (t, $J = 7.7$ Hz, 2H), 7.15 (d, $J = 7.7$ Hz, 4H), 7.04 (d, $J = 8.5$ Hz, 2H), 7.00-6.89 (m, 8H), 4.74 (dd, $J = 12.4, 6.7$ Hz, 1H), 4.60 (dd, $J = 12.4, 7.9$ Hz, 1H), 4.10 (p, $J = 7.1$ Hz, 1H), 3.35 (qd, $J = 17.6, 6.9$ Hz, 2H); ^{13}C NMR (101 MHz, CDCl_3 , ppm): $\delta = 196.01, 146.48, 146.38, 135.42, 132.52, 131.56, 128.25, 127.72, 127.17, 127.03, 123.46, 122.65, 122.03, 78.59, 40.57, 37.74$; MS (MALDI-TOF): calculated for $\text{C}_{28}\text{H}_{24}\text{N}_2\text{O}_3$ $[\text{M}+\text{H}]^+ = 437.1787$ m/z , found 437.1787 m/z .

1-(4-(diphenylamino)phenyl)-4-nitro-3-phenylbutan-1-one (Compound 8):

Following the procedure for Compound 7 described above, using Compound 5 (1.67 g, 4.53 mmol) as starting materials. The residue was separated by column chromatography (petroleum ether: $\text{CH}_2\text{Cl}_2 = 1:1$) to afford an orange solid (1.79 g, yield: 90.8%); ^1H NMR (400 MHz, CDCl_3 , ppm): $\delta = 7.86$ (d, $J = 7.9$ Hz, 2H), 7.51 (t, $J = 7.4$ Hz, 1H), 7.40 (t, $J = 7.7$ Hz, 2H), 7.19 – 7.12 (m, 4H), 7.05 (d, $J = 8.6$ Hz, 2H), 7.00-6.91 (m, 8H), 4.74 (dd, $J = 12.4, 6.7$ Hz, 1H), 4.60 (dd, $J = 12.4, 8.0$ Hz, 1H), 4.16-4.04 (m, 1H), 3.36 (qd, $J = 17.6, 6.9$ Hz, 2H); ^{13}C NMR (101 MHz, CDCl_3 , ppm): $\delta = 196.01, 146.47, 146.37, 135.41, 132.52, 131.55, 128.25, 127.71, 127.17, 127.03, 123.45, 122.64, 122.02, 78.59, 40.57, 37.73$; HRMS (ESI): calculated for $\text{C}_{28}\text{H}_{24}\text{N}_2\text{O}_3$ $[\text{M}+\text{H}]^+ = 437.1787$ m/z , found 437.1783 m/z .

1,3-bis(4-(diphenylamino)phenyl)-4-nitrobutan-1-one (Compound 9): Following the procedure for Compound 7 described above, using Compound 6 (1.51 g, 2.76 mmol, 1.0 eq), nitromethane (1.68 g, 27.60 mmol, 10.0 eq), and diethylamine (2.02 g, 33.61 mmol, 12.2 eq) as starting materials. The crude product was recrystallized with CH_2Cl_2 and *n*-hexane to obtain an orange-red solid (1.56 g), directly used in next step without further purification; MS (MALDI-TOF): calculated for $\text{C}_{40}\text{H}_{33}\text{N}_3\text{O}_3$ $[\text{M}]^+ = 604.2522$ m/z , found 604.2521 m/z .

(Z)-4-(2-((3-(4-(diphenylamino)phenyl)-5-phenyl-1H-pyrrol-2-yl)imino)-5-phenyl-2H-pyrrol-3-yl)-N,N-diphenylaniline (Compound 10): Compound 7 (2.00 g, 4.58 mmol), ammonium acetate (12.83 g, 166.47 mmol) and *n*-butanol (15 mL) were mixed in a two-necked flask (100 mL). The reaction mixture was stirred at 110 °C for 24 h under N_2 . After the reaction was completed, the reaction system was cooled to

room temperature. The reaction mixture was filtered and the filter cake was obtained as a crude product. The crude product was dissolved in CH₂Cl₂ (30 mL), then washed with water (50 mL × 3). The resulting organic layer was washed with brine and dried with anhydrous magnesium sulfate. After removing the solvents by evaporation, the resulting crude mixture was separated by column chromatography (petroleum ether:CH₂Cl₂ = 2:3) to afford a purple solid (1.53 g, yield: 76%); ¹H NMR (400 MHz, CDCl₃, ppm): δ = 7.96 – 7.90 (m, 8H), 7.50 (t, *J* = 7.4 Hz, 4H), 7.44 (dd, *J* = 8.3, 6.3 Hz, 2H), 7.19 (dd, *J* = 11.1, 4.6 Hz, 9H), 7.14-7.09 (m, 8H), 7.06 (dd, *J* = 9.1, 6.6 Hz, 6H), 6.99 (dd, *J* = 10.2, 4.2 Hz, 4H); ¹³C NMR (101 MHz, CDCl₃, ppm): δ = 154.93, 149.78, 147.69, 147.42, 142.30, 132.32, 129.91, 129.84, 129.25, 129.09, 127.96, 126.50, 124.53, 123.17, 123.09, 113.48; HRMS (ESI): calculated for C₅₆H₄₁N₅ [M+H]⁺ = 784.3362 *m/z*, found, 783.3362 *m/z*.

(Z)-4-(2-((5-(4-(diphenylamino)phenyl)-3-phenyl-1H-pyrrol-2-yl)imino)-3-phenyl-2H-pyrrol-5-yl)-N,N-diphenylaniline (Compound 11): Following the procedure for Compound **10** described above, using Compound **8** (2.00 g, 4.58 mmol), ammonium acetate (20.03 g, 259.46 mmol) and *n*-butanol (15 mL) as starting materials. The residue was separated by column chromatography (petroleum ether:CH₂Cl₂ = 1:1) to afford a purple solid Compound **11** (1.56 g, yield: 78%); ¹H NMR (400 MHz, CDCl₃, ppm): δ = 8.04 (t, *J* = 8.4 Hz, 8H), 7.49-7.37 (m, 6H), 7.32 (t, *J* = 7.8 Hz, 8H), 7.19 (d, *J* = 7.7 Hz, 8H), 7.13 (t, *J* = 7.3 Hz, 4H), 7.08 (d, *J* = 9.4 Hz, 4H), 7.04 (s, 2H); ¹³C NMR (101 MHz, CDCl₃, ppm): δ = 153.90, 148.76, 146.66, 146.39, 141.27, 131.30, 128.88, 128.82, 128.23, 128.07, 126.94, 125.47, 123.51, 122.14, 122.07, 112.46; HRMS (ESI): calculated for C₅₆H₄₁N₅ [M+H]⁺ = 783.3362 *m/z*, found 783.3362 *m/z*.

(Z)-4,4'-(2-((3,5-bis(4-(diphenylamino)phenyl)-1H-pyrrol-2-yl)imino)-2H-pyrrole-3,5-diyl)bis(N,N-diphenylaniline) (Compound 12): Following the procedure for Compound **10** described above, using Compound **9** (2.00 g, 4.58 mmol), ammonium acetate (20.03 g, 259.46 mmol) and *n*-butanol (15 mL) as starting materials. The residue was separated by column chromatography (petroleum ether:CH₂Cl₂ = 2:3) to afford a deep purple solid Compound **12** (0.40 g, yield: 21.8 %); ¹H NMR (400 MHz, CDCl₃,

ppm): $\delta = 7.94$ (d, $J = 8.5$ Hz, 4H), 7.75 (d, $J = 8.5$ Hz, 4H), 7.29 (t, $J = 7.7$ Hz, 8H), 7.17 (dd, $J = 13.6, 7.6$ Hz, 16H), 7.11 (d, $J = 7.9$ Hz, 14H), 7.07 (d, $J = 6.2$ Hz, 4H), 7.03 (d, $J = 3.8$ Hz, 4H), 6.98 (t, $J = 7.1$ Hz, 5H); ^{13}C NMR(101 MHz, CDCl_3 , ppm): $\delta = 149.77, 148.64, 147.57, 147.50, 147.44, 147.39, 147.01, 133.69, 129.81, 129.51, 129.44, 127.96, 127.84, 127.48, 125.56, 125.27, 124.90, 124.67, 124.43, 123.93, 123.50, 123.34, 123.29, 123.19, 123.16, 123.06, 122.46, 115.30$; MS (MALDI-TOF): calculated for $\text{C}_{80}\text{H}_{59}\text{N}_7$ $[\text{M}+\text{H}]^+ = 1118.4832$ m/z , found 1118.4832 m/z .

Aza-BODIPY 1: The compound **10** (1.08 g, 1.38 mmol, 1.0 eq) was dissolved in dry CH_2Cl_2 (60 mL) under N_2 atmosphere and DIEA (2.87 mg, 16.56 mmol, 12.2 eq) was added and stirred. After 30 minutes, $\text{BF}_3\text{-OEt}_2$ (2.87 ml, 23.736 mmol, 17.2 eq) was added, and stirred at room temperature for 24h under N_2 protection. After the reaction, it was rinsed with saturated NH_4Cl , NaCl and water respectively, dried with anhydrous Na_2SO_4 , concentrated under reduced pressure to obtain crude products, separated and purified by column chromatography (petroleum ether: dichloromethane = 2:1), and obtained 0.89 g of green-black solid (yield: 78%); m. p. 298 $^\circ\text{C}$; ^1H NMR (400 MHz, CDCl_3): $\delta = 8.00$ (s, 4H), 7.95 (d, $J = 8.8$ Hz, 4H), 7.45 (d, $J = 6.7$ Hz, 6H), 7.22 (d, $J = 7.4$ Hz, 8H), 7.15 (d, $J = 7.5$ Hz, 8H), 7.06 (dd, $J = 14.0, 8.0$ Hz, 8H), 6.87 (s, 2H); ^{13}C NMR (101 MHz, CDCl_3): $\delta = 158.66, 149.13, 146.93, 145.64, 143.39, 132.06, 130.46, 130.36, 128.48, 126.01, 125.27, 123.99, 121.92, 116.87, 26.93$; HRMS (ESI): calculated for $\text{C}_{56}\text{H}_{40}\text{BF}_2\text{N}_5$ $[\text{M}+\text{H}]^+ = 831.3345$ m/z , found 832.3345 m/z ; UV/Vis (CH_2Cl_2): $\lambda_{\text{max}}(\epsilon) = 759$ (33700), 649 nm (40700 $\text{M}^{-1} \text{cm}^{-1}$), 321 nm (53000 $\text{M}^{-1} \text{cm}^{-1}$); fluorescence (CH_2Cl_2): $\lambda_{\text{max}} = 797$ nm; quantum yield (CH_2Cl_2): $\Phi = 0.065$; fluorescence lifetime (CH_2Cl_2): $\tau = 1.8$ ns.

Aza-BODIPY 2: Using crude product **11** (4 g) as raw material, according to the same experimental procedure of aza-BODIPY **1**, blue-black solid was obtained (2.08 g, yield: 50%); m. p. 293 $^\circ\text{C}$; ^1H NMR (400 MHz, CDCl_3): $\delta = 8.04$ (t, $J = 8.4$ Hz, 8H), $7.48 - 7.37$ (m, 6H), 7.32 (t, $J = 7.8$ Hz, 8H), 7.19 (d, $J = 7.7$ Hz, 8H), 7.13 (t, $J = 7.3$ Hz, 4H), 7.08 (d, $J = 9.4$ Hz, 4H), 7.04 (s, 2H); ^{13}C NMR (101 MHz, CDCl_3): $\delta = 156.54, 150.17, 146.51, 145.47, 141.99, 132.76, 131.13, 129.57, 129.20, 128.91, 128.48, 126.06,$

124.57, 123.76, 120.31, 118.55; HRMS (ESI): calculated for $C_{56}H_{40}BF_2N_5$ $[M+H]^+ = 831.3345$ m/z , found 832.3345 m/z ; UV/Vis (CH_2Cl_2): $\lambda_{max}(\epsilon) = 800$ (72800), 576 nm (30500 $M^{-1} cm^{-1}$), 339 nm (38600 $M^{-1} cm^{-1}$); fluorescence (CH_2Cl_2): $\lambda_{max} = 867$ nm; quantum yield (CH_2Cl_2): $\Phi = 0.116$; fluorescence lifetime (CH_2Cl_2): $\tau = 1.8$ ns.

Aza-BODIPY 3: Using crude product **12** (0.98 g) as raw material, according to the same experimental procedure of aza-BODIPY **1**, blue-black solid was obtained (0.78 g, yield: 75%); m. p. 292 °C; 1H NMR (400 MHz, $CDCl_3$): $\delta = 8.00$ (d, $J = 8.9$ Hz, 4H), 7.93 (d, $J = 8.7$ Hz, 4H), 7.31 (t, $J = 7.8$ Hz, 8H), 7.24 – 7.16 (m, 16H), 7.12 (dd, $J = 11.7, 7.4$ Hz, 12H), 7.04 (dd, $J = 8.7, 4.3$ Hz, 12H), 6.94 (s, 2H); ^{13}C NMR (101 MHz, $CDCl_3$): $\delta = 156.18, 149.86, 148.59, 147.13, 146.64, 145.47, 141.50, 130.90, 130.08, 129.52, 129.36, 126.52, 125.95, 125.04, 124.38, 124.23, 123.68, 122.28, 120.45, 116.63$; HRMS: calculated for $C_{80}H_{58}BF_2N_7$ $[M + H]^+ = 1166.4906$ m/z , found 1166.4906 m/z . UV/Vis (CH_2Cl_2): $\lambda_{max}(\epsilon) = 820$ (80800), 647 nm (38400 $M^{-1} cm^{-1}$), 307 nm (64500 $M^{-1} cm^{-1}$); fluorescence (CH_2Cl_2): $\lambda_{max} = 892$ nm; quantum yield (CH_2Cl_2): $\Phi = 0.209$. fluorescence lifetime (CH_2Cl_2): $\tau = 3.5$ ns.

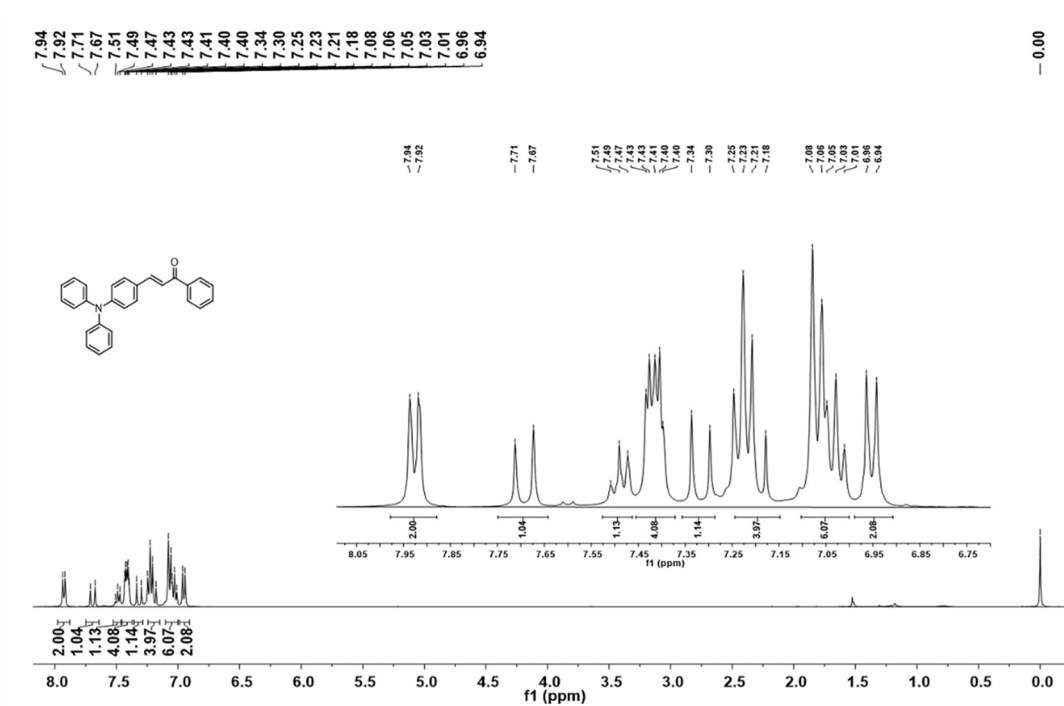


Fig S1. The ¹H NMR spectrum and chemical structure of compound **4** in CDCl₃.

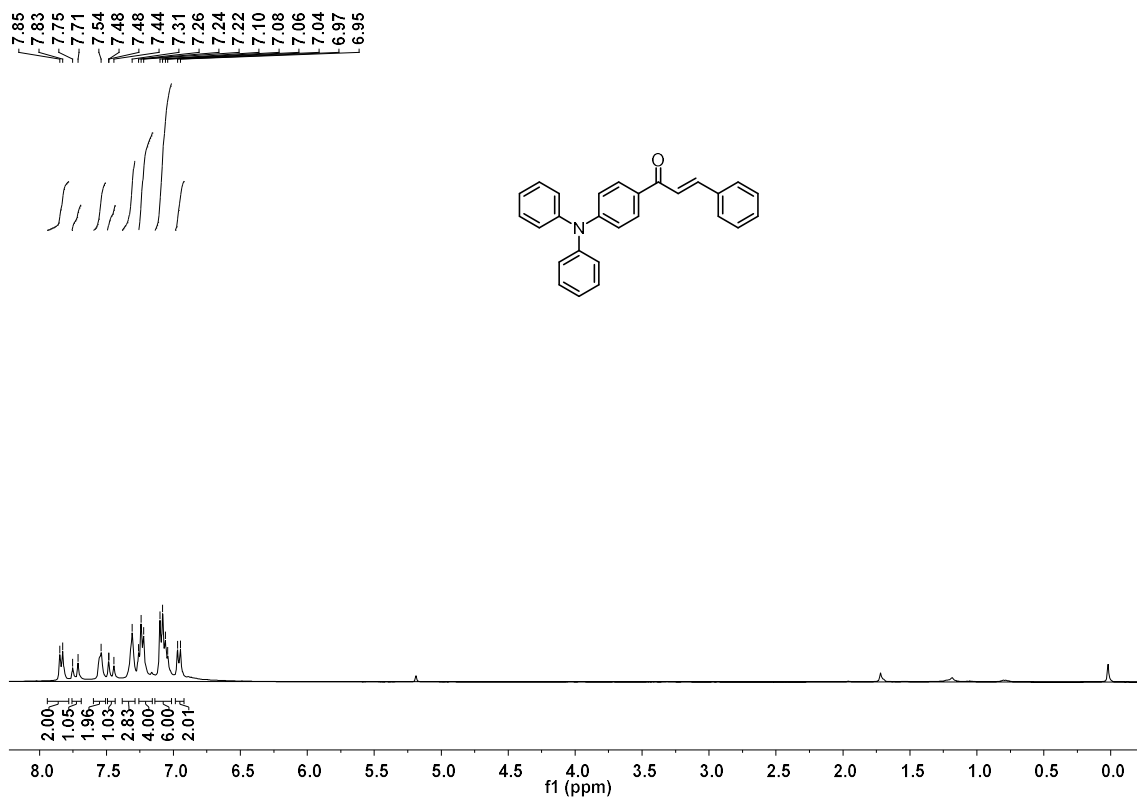


Fig S2. ¹H NMR spectrum and chemical structure of compound 5 in CDCl₃.

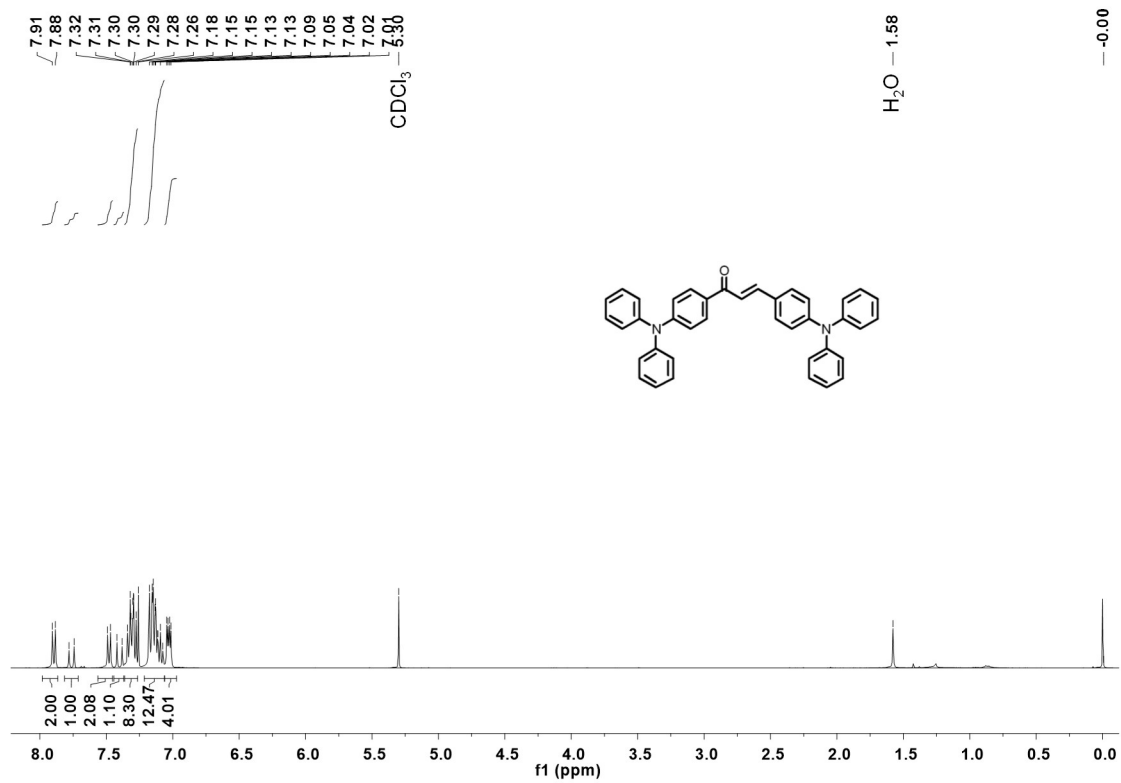


Fig S3. ¹H NMR spectrum and chemical structure of compound **6** in CDCl₃.

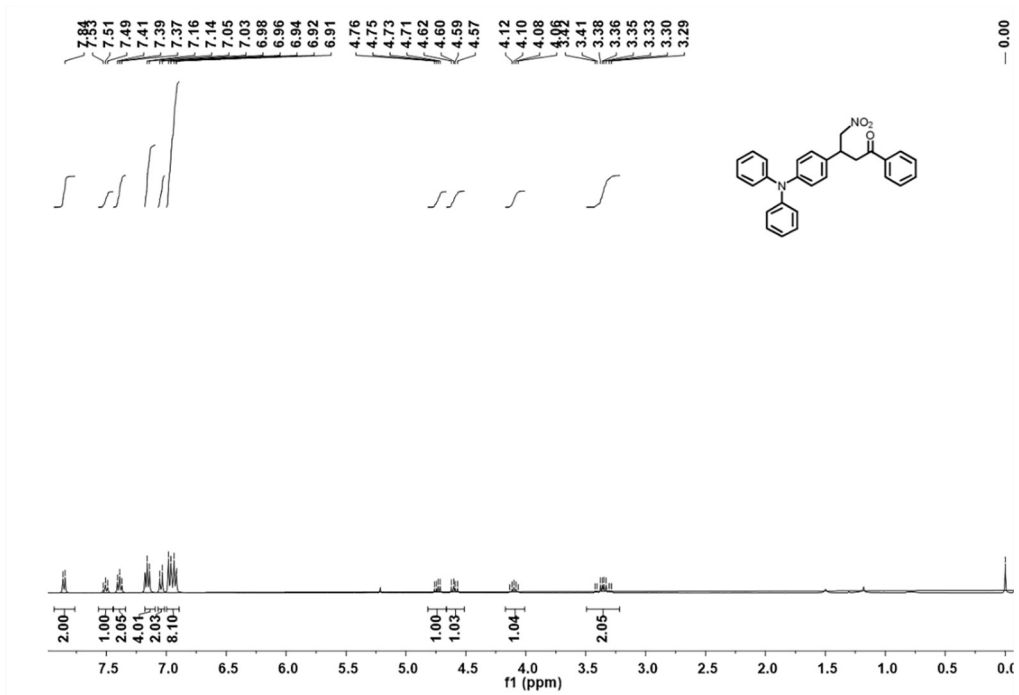


Fig S4. ^1H NMR spectrum and chemical structure of compound **7** in CDCl_3 .

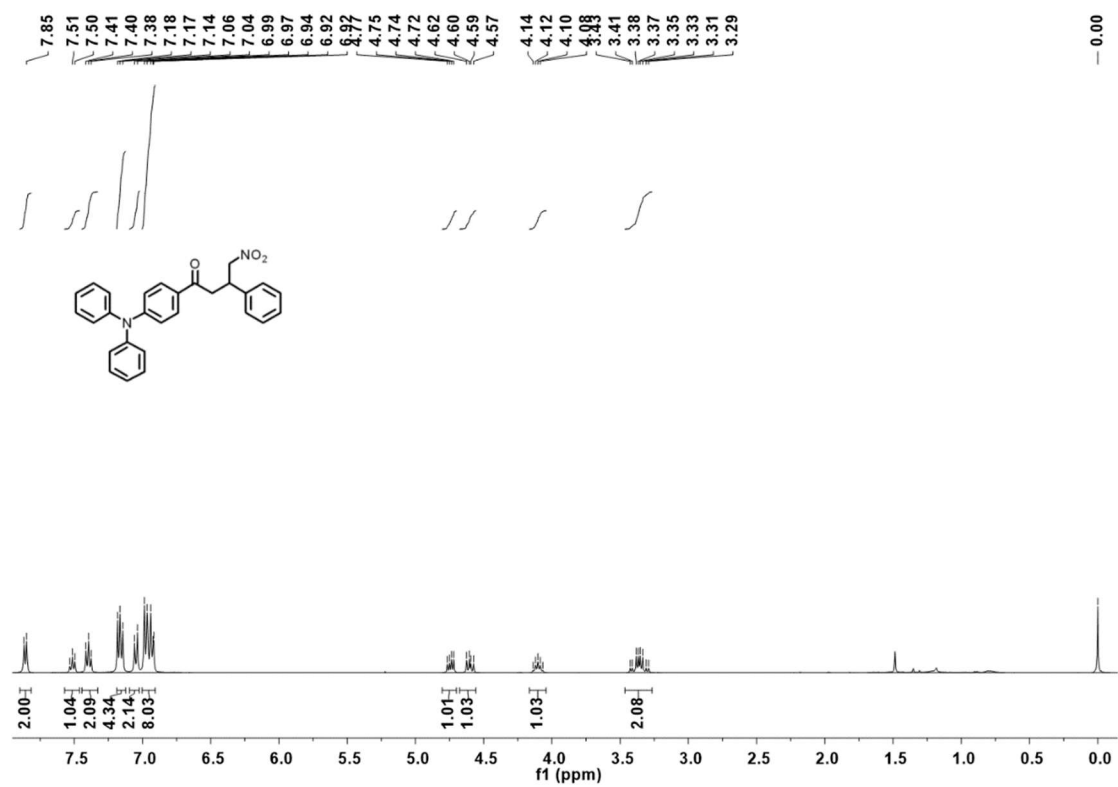


Fig S5. ¹H NMR spectrum and chemical structure of compound **8** in CDCl₃.

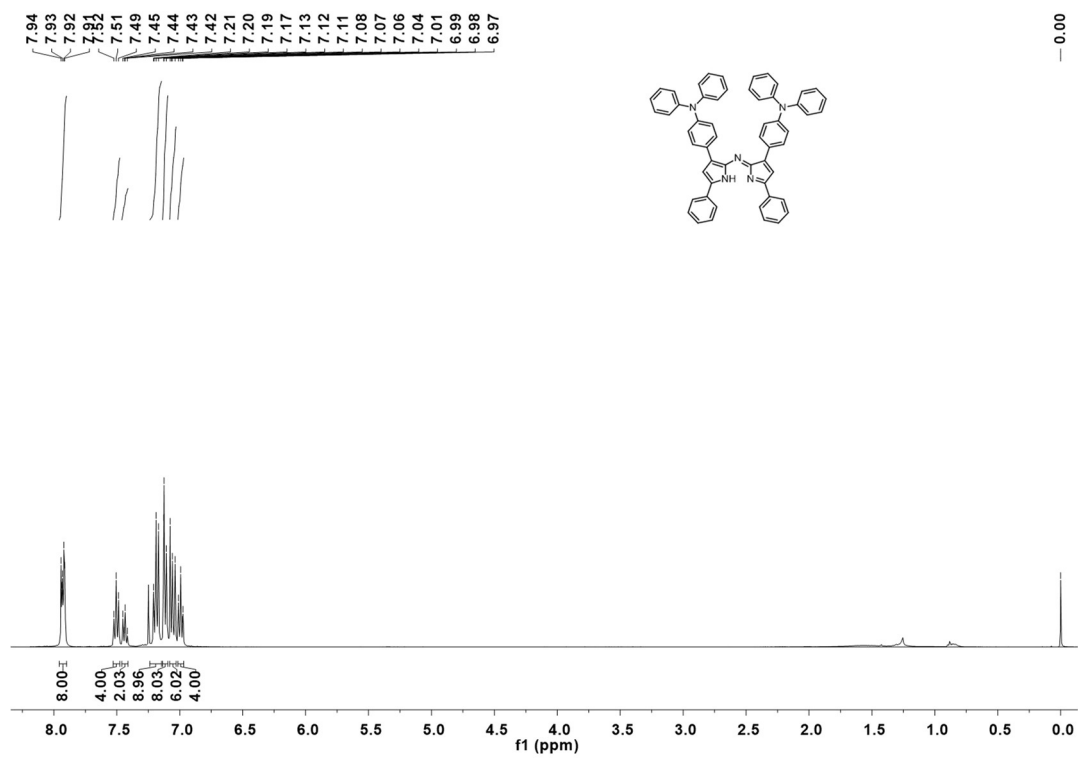


Fig S6. ¹H NMR spectrum and chemical structure of compound **10** in CDCl₃.

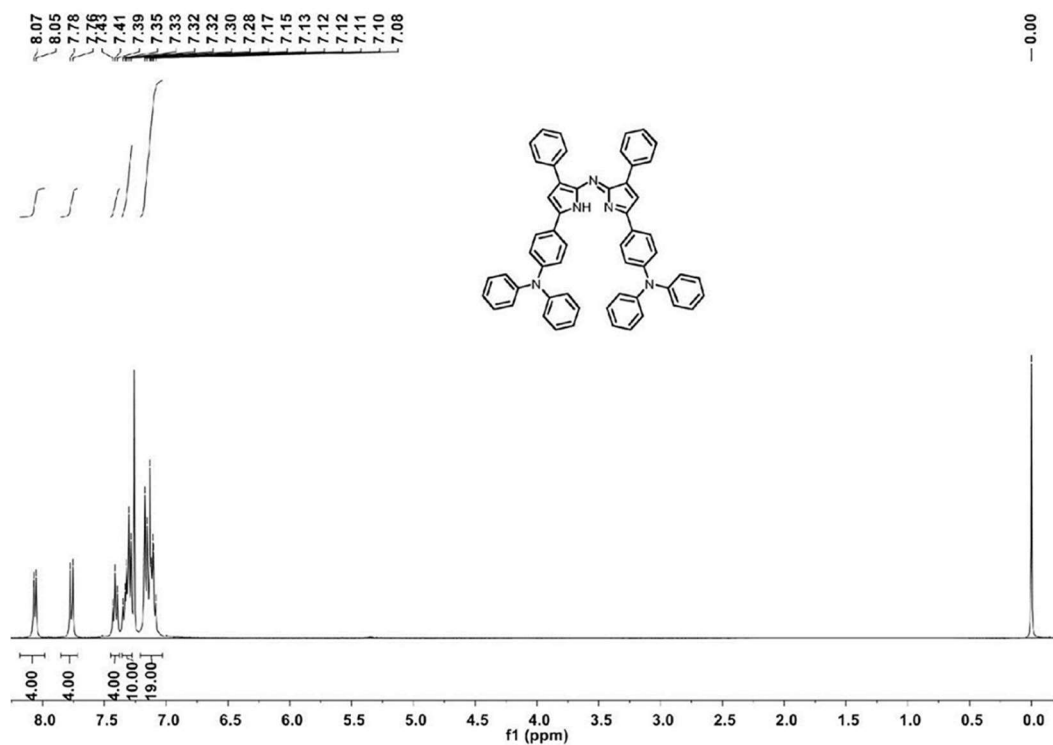


Fig S7. ¹H NMR spectrum and chemical structure of compound **11** in CDCl₃.

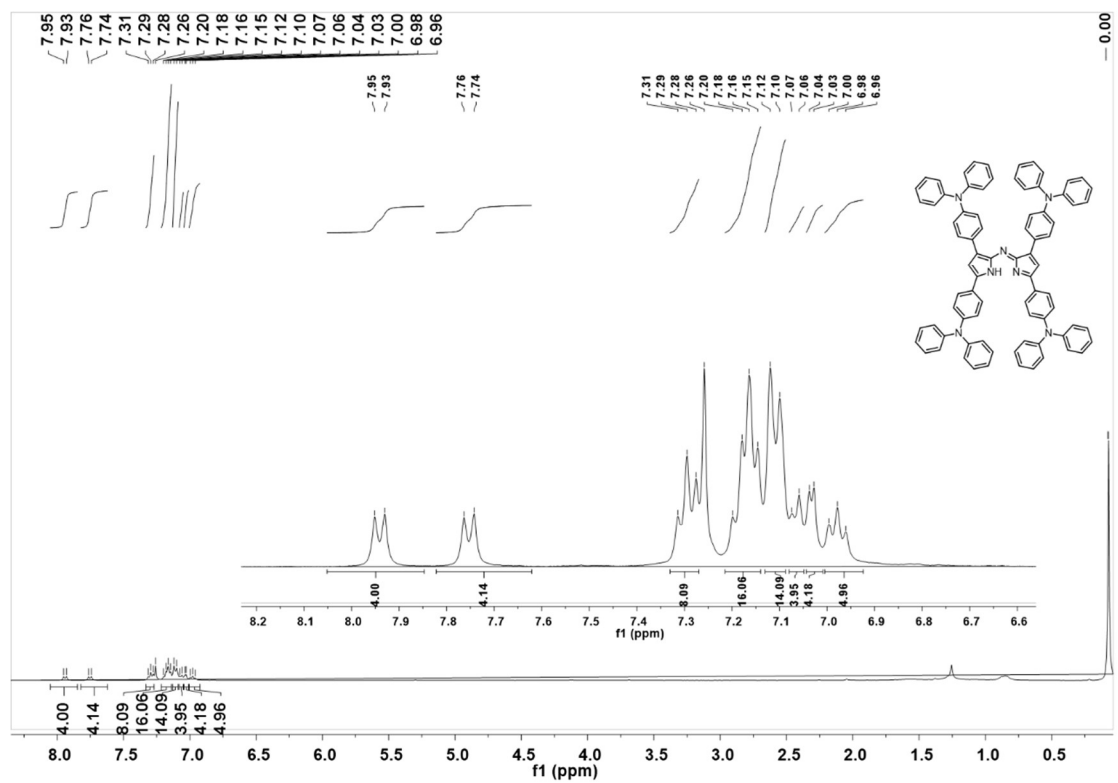


Fig S8. ^1H NMR spectrum and chemical structure of compound **12** in CDCl_3 .

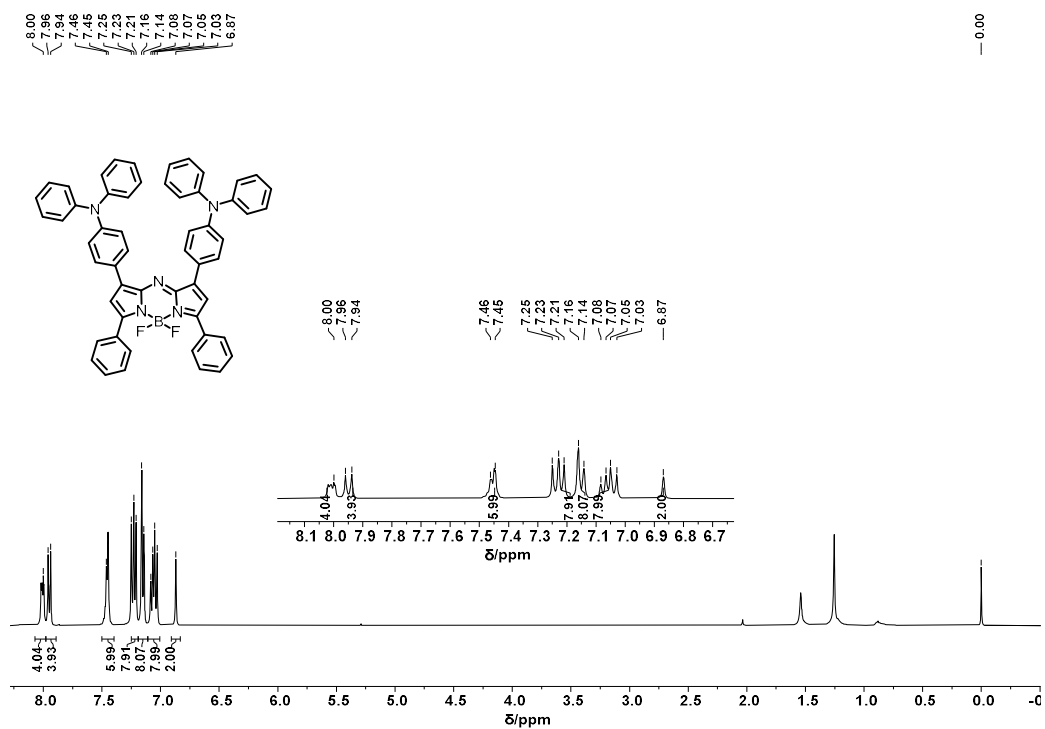


Fig S9. ^1H NMR spectrum and chemical structure of aza-BODIPY 1 in CDCl₃ solution.

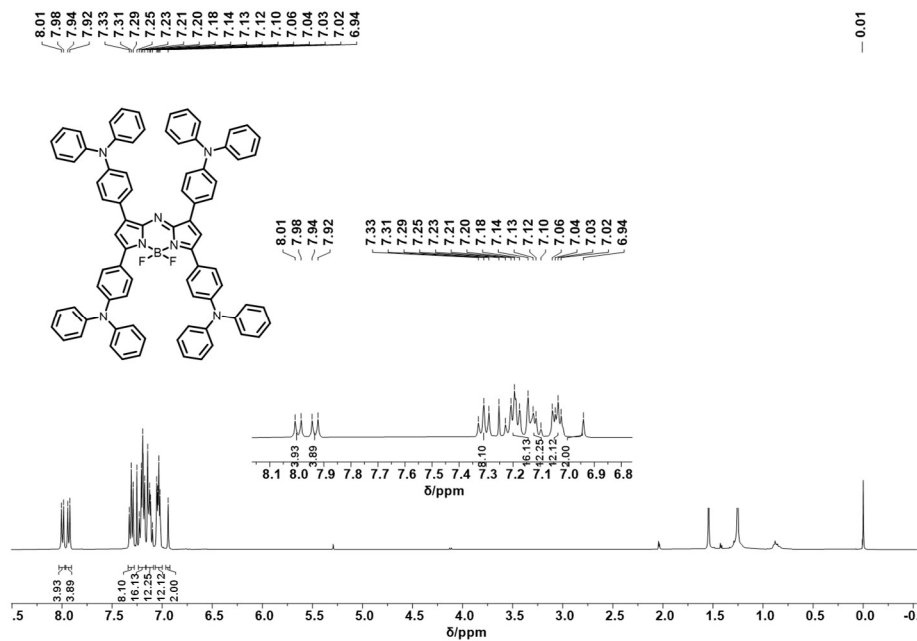


Fig S11. ¹H NMR spectrum and chemical structure of aza-BODIPY 3 in CDCl₃ solution.

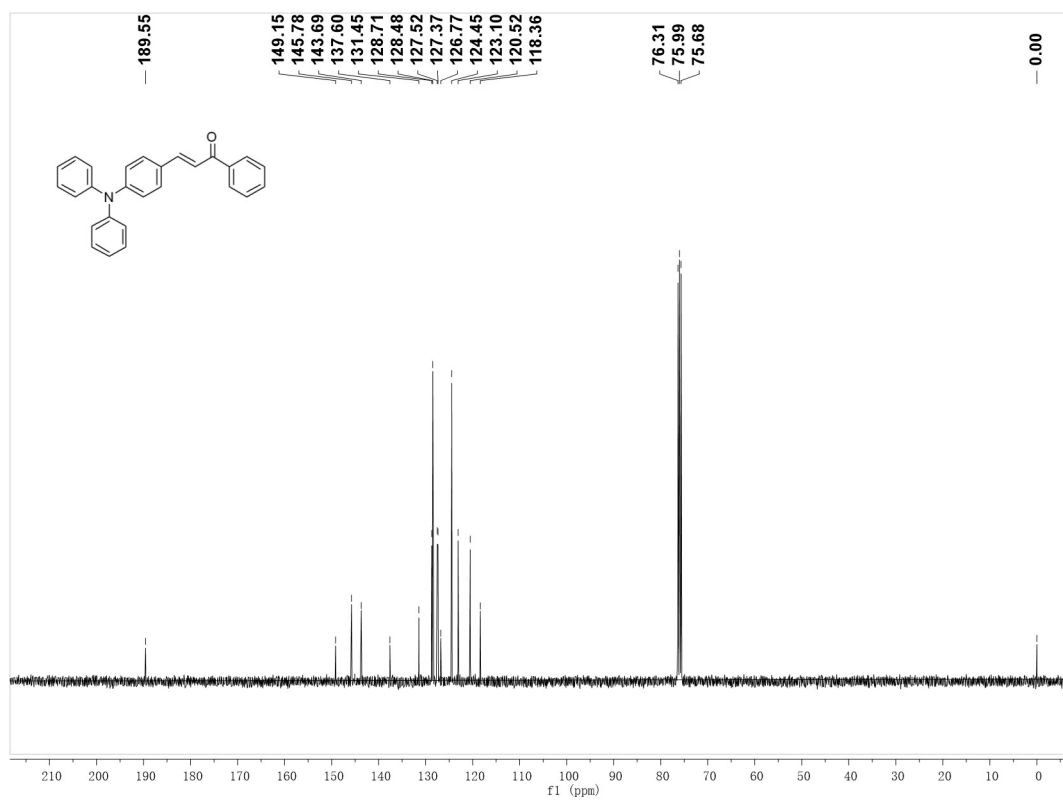


Fig S12. ^{13}C NMR spectrum and chemical structure of compound 4 in CDCl_3 .

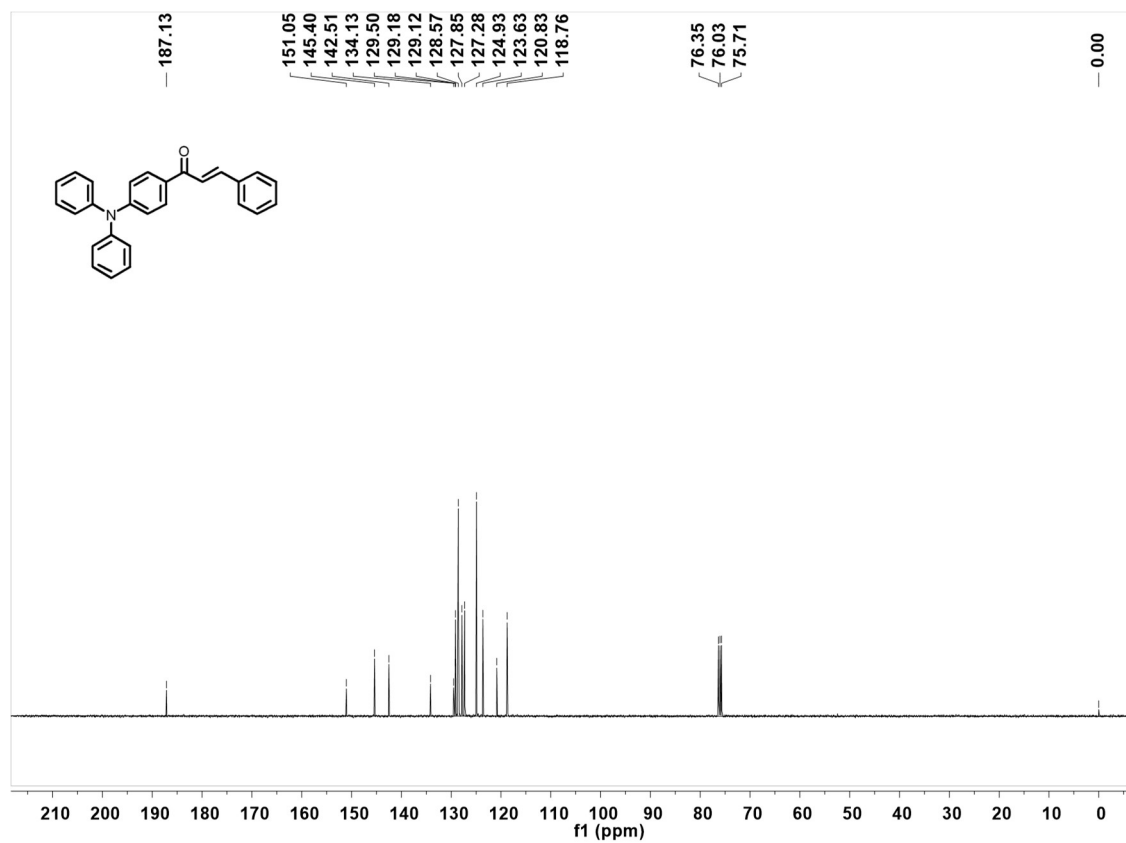


Fig S13. ^{13}C NMR spectrum and chemical structure of compound **5** in CDCl_3 .

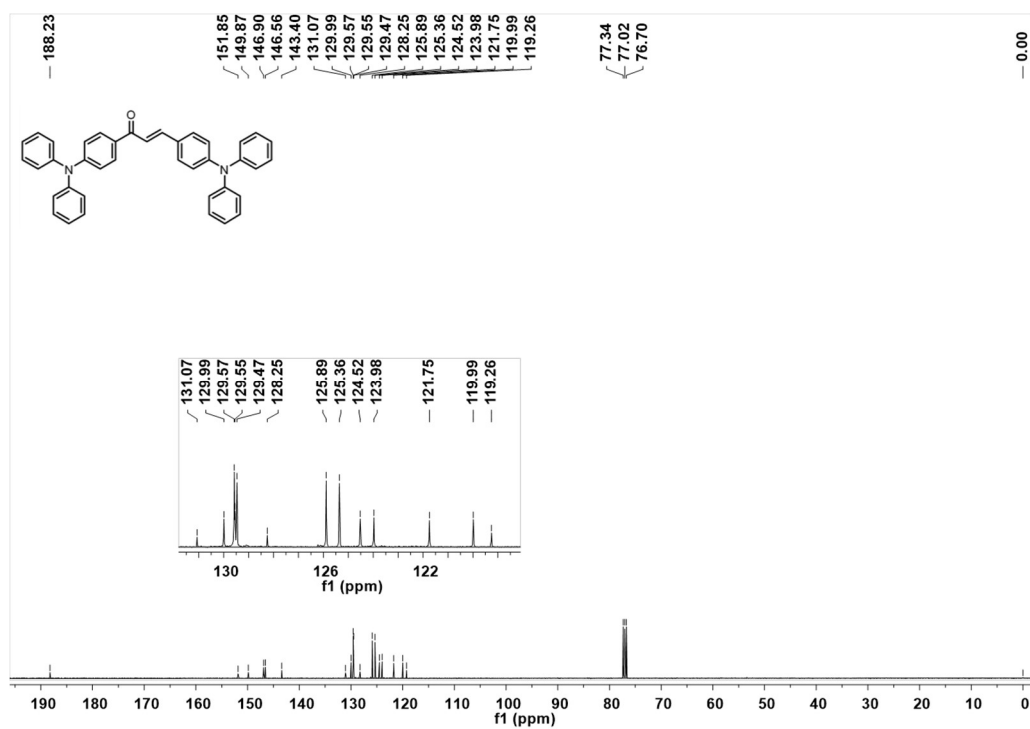


Fig S14. ^{13}C NMR spectrum and chemical structure of compound **6** in CDCl_3 .

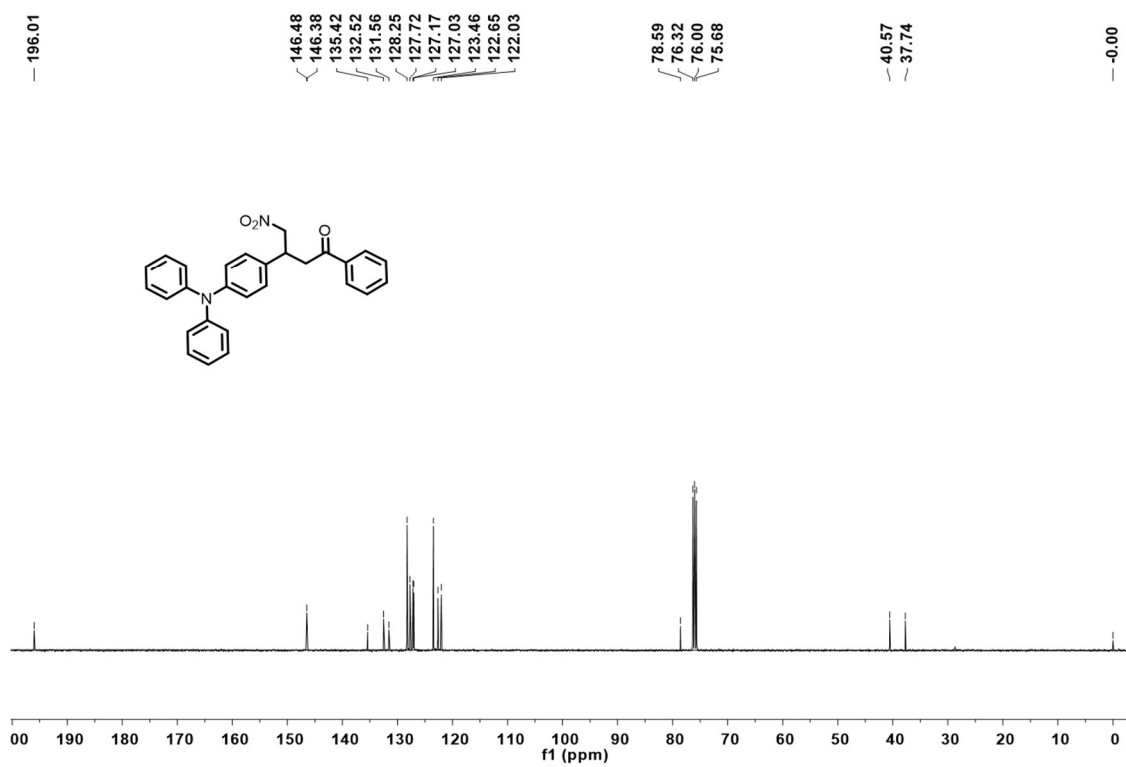


Fig S15. ^{13}C NMR spectrum and chemical structure of compound **7** in CDCl_3 .

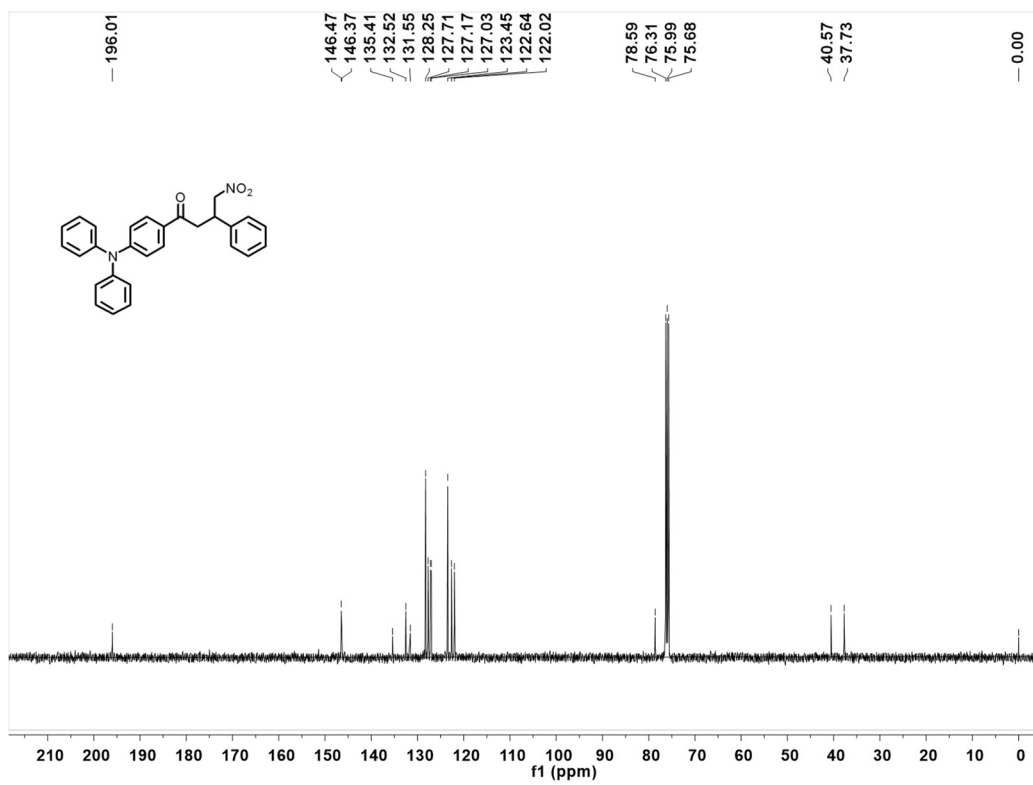


Fig S16. ¹³C NMR spectrum and chemical structure of compound **8** in CDCl₃.

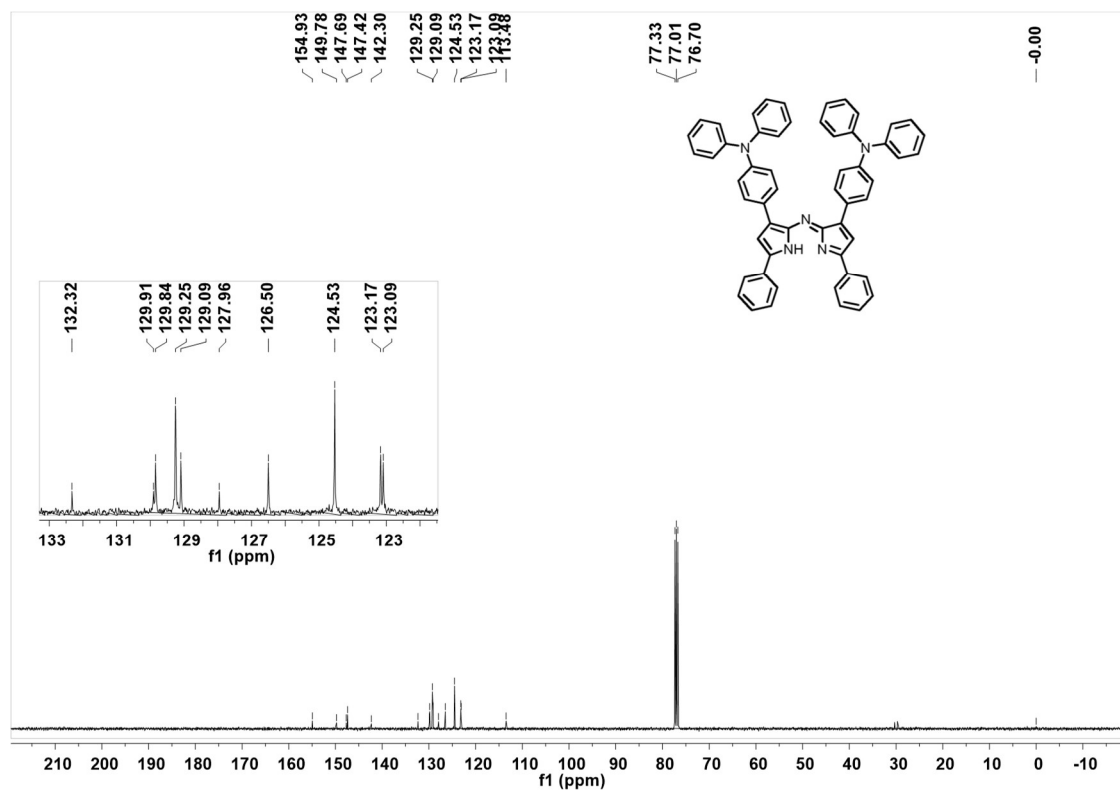


Fig S17. ^{13}C NMR spectrum and chemical structure of compound **10** in CDCl_3 .

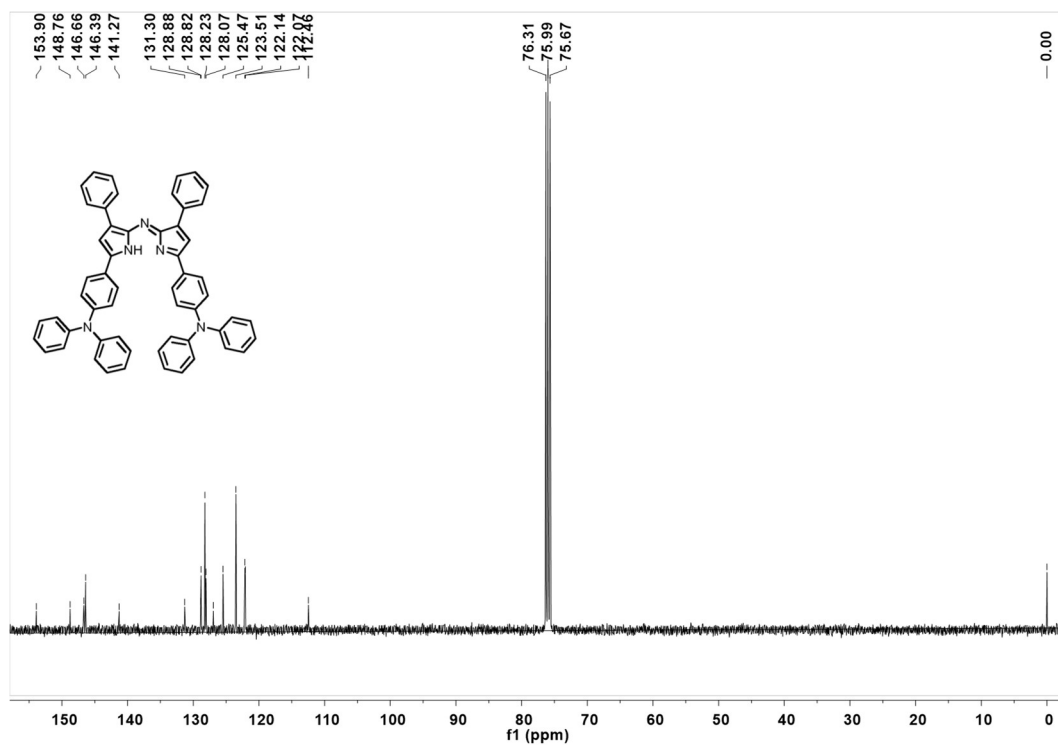


Fig S18. ^{13}C NMR spectrum and chemical structure of compound **11** in CDCl_3 .

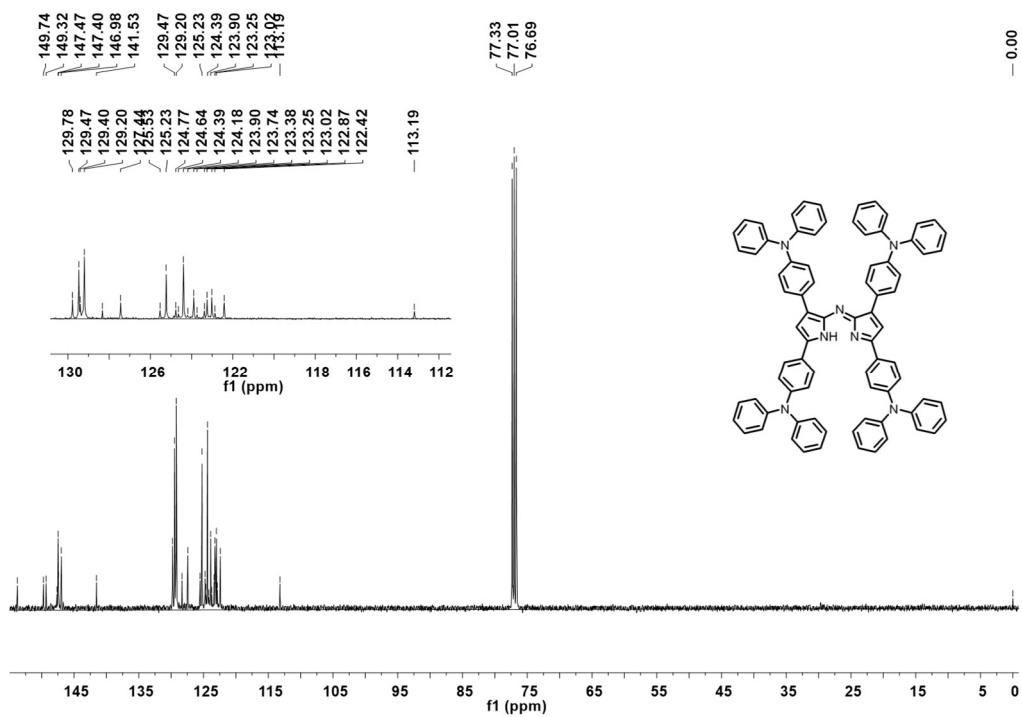


Fig S19. ^{13}C NMR spectrum and chemical structure of compound **12** in CDCl_3 .

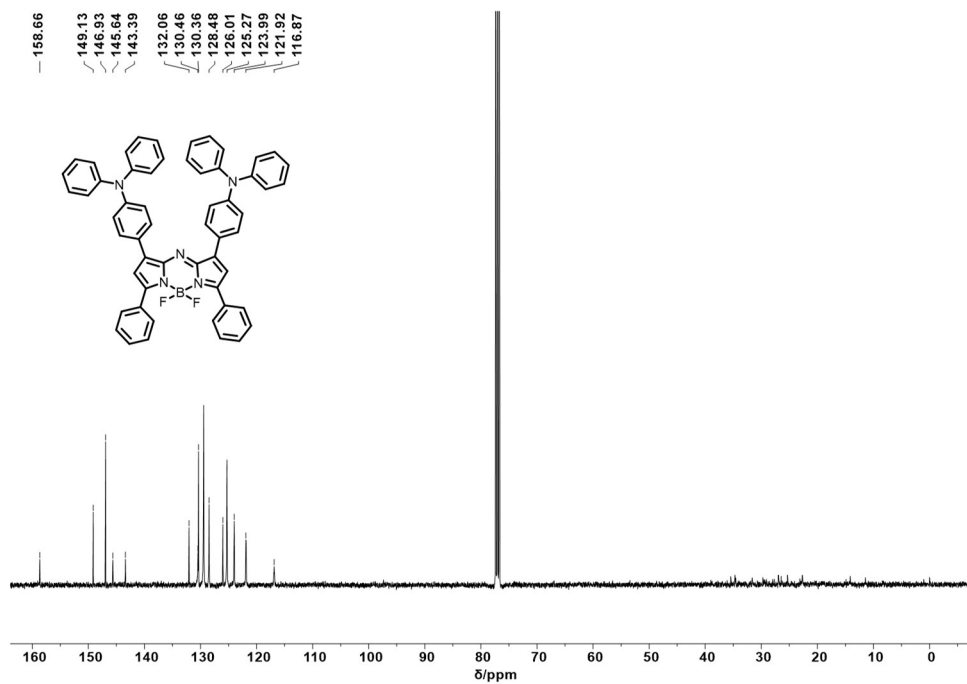


Fig S20. ^{13}C NMR spectrum and chemical structure of aza-BODIPY **1** in CDCl_3 solution

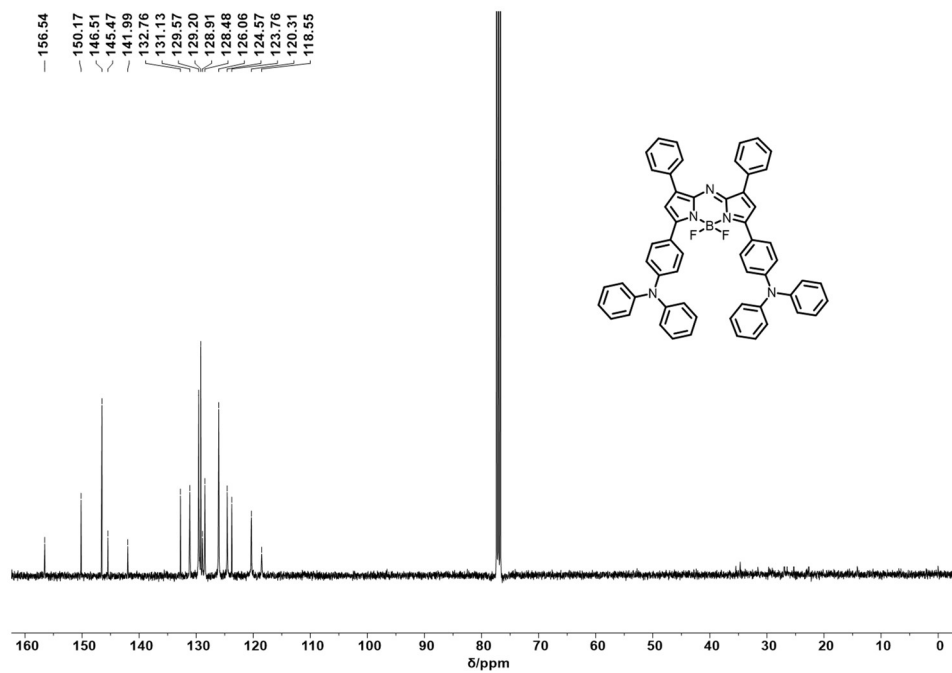


Fig S21. ^{13}C NMR spectrum and chemical structure of aza-BODIPY **2** in CDCl_3 solution.

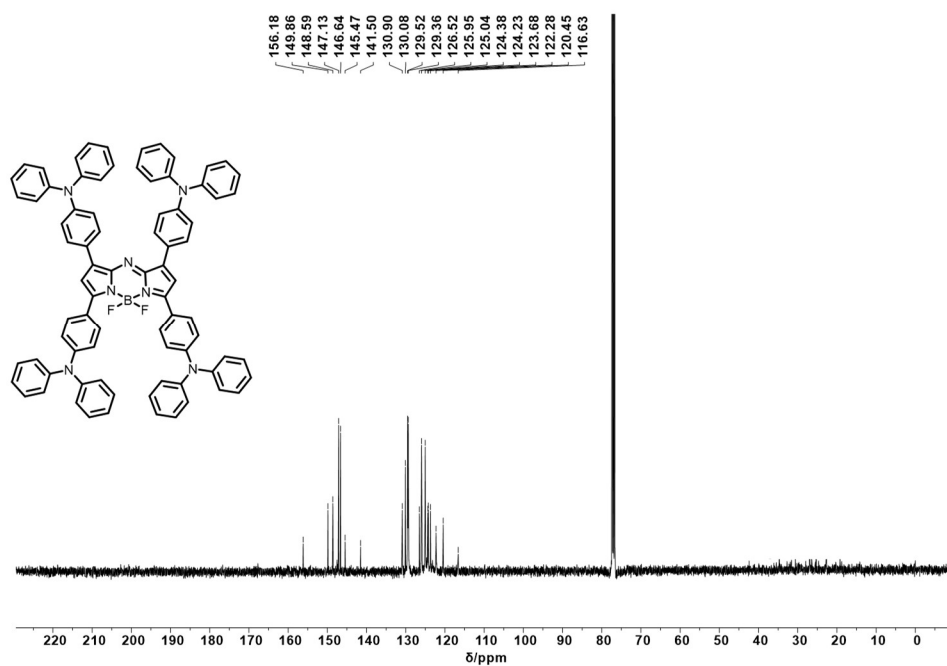


Fig S22. ¹³C NMR spectrum and chemical structure of aza-BODIPY 3 in CDCl₃ solution.

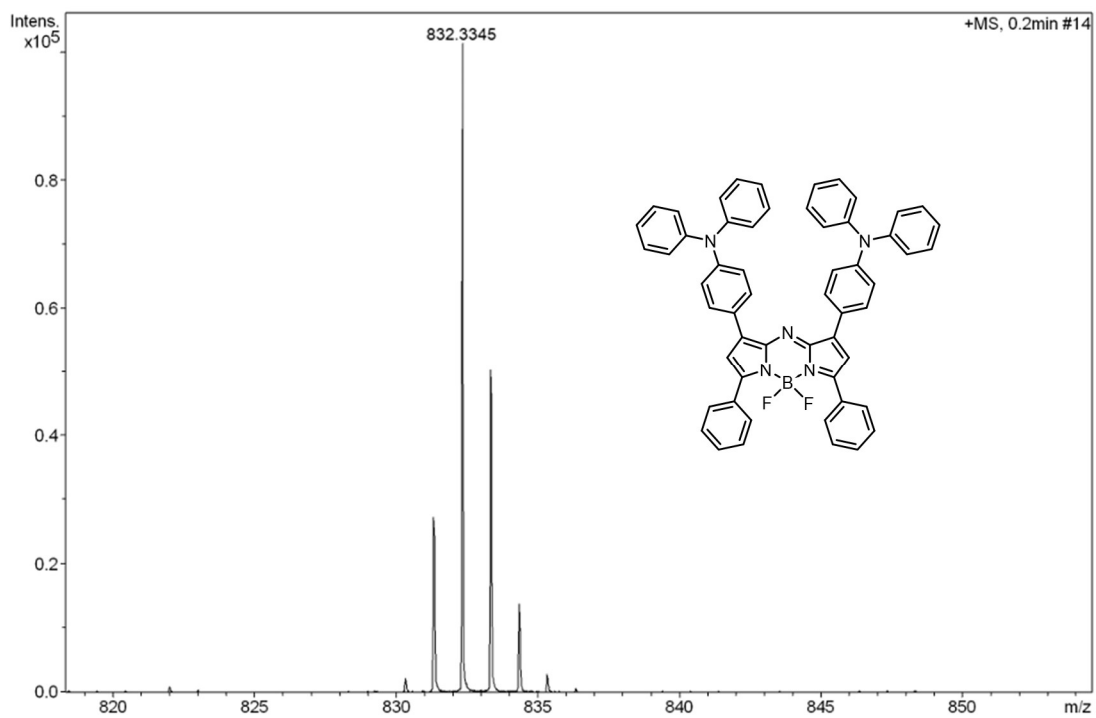


Fig S23. HRMS spectrum of aza-BODIPY 1.

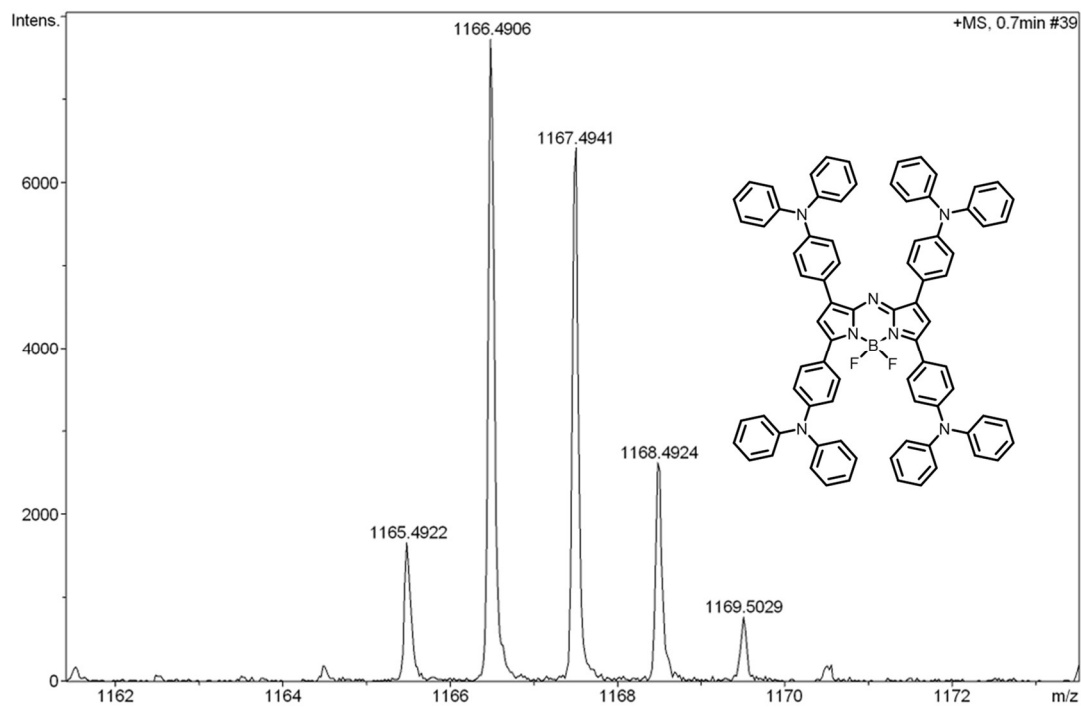


Fig S25. HRMS spectrum and chemical structure of aza-BODIPY 3.

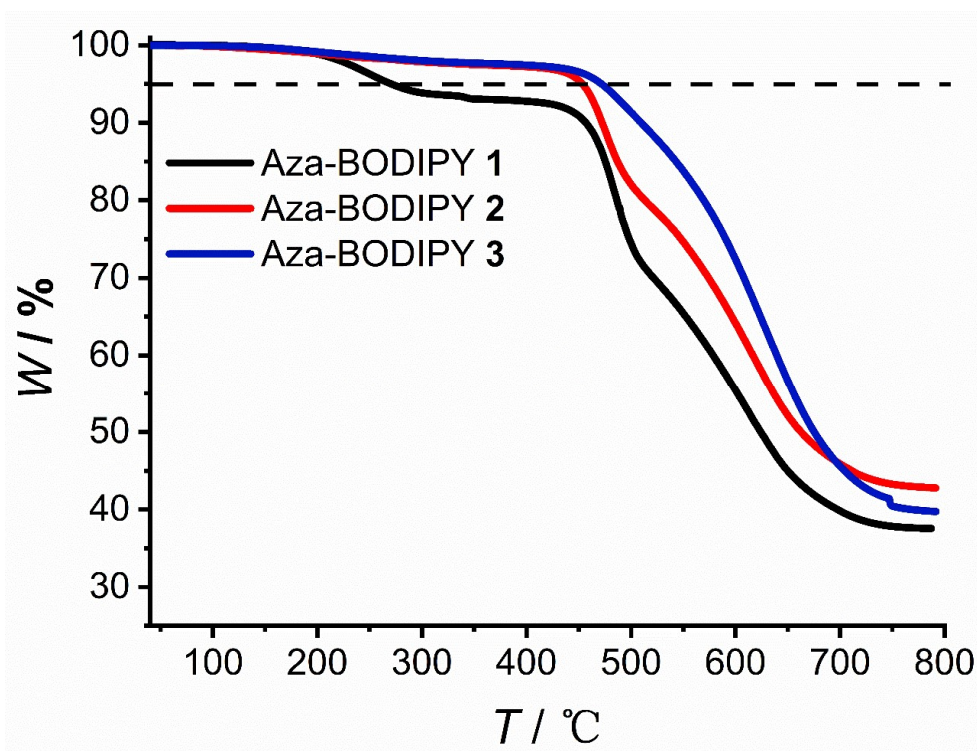


Fig S26. Thermal gravimetric (TGA) curves at a heating rate of $20\text{ }^{\circ}\text{C min}^{-1}$ in Ar of aza-BODIPY 1-3.

Table S1. Crystal data for aza-BODIPY 1.

Empirical formula	C ₅₆ H ₄₀ BF ₂ N ₅
Formula weight	831.74
Temperature/K	113.15
Crystal system	triclinic
Space group	<i>P</i> -1
<i>a</i> /Å	10.25300(10)
<i>b</i> /Å	14.6147(2)
<i>c</i> /Å	15.2446(2)
α /°	95.0590(10)
β /°	105.9420(10)
γ /°	98.4550(10)
Volume/Å ³	2152.65(5)
<i>Z</i>	2
ρ_{calc} /cm ³	1.283
μ /mm ⁻¹	0.081
F(000)	868.0
Crystal size/mm ³	0.29 × 0.24 × 0.15
Radiation	Mo K α (λ = 0.71073)
2 Θ range for data collection/°	3.714 to 56.562
Index ranges	-13 ≤ <i>h</i> ≤ 13, -19 ≤ <i>k</i> ≤ 17, -20 ≤ <i>l</i> ≤ 20
Reflections collected	42501
Independent reflections	10609 [<i>R</i> _{int} = 0.0476, <i>R</i> _{sigma} = 0.0458]
Data/restraints/parameters	10609/1/577
Goodness-of-fit on F ²	1.047
Final <i>R</i> indexes [<i>I</i> ≥ 2 σ (<i>I</i>)]	<i>R</i> ₁ = 0.0520, <i>wR</i> ₂ = 0.1139
Final <i>R</i> indexes [all data]	<i>R</i> ₁ = 0.0728, <i>wR</i> ₂ = 0.1277
Largest diff. peak/hole / e Å ⁻³	0.27/-0.25

Table S2. Crystal data for aza-BODIPY 2.

Empirical formula	C ₅₆ H ₄₀ BF ₂ N ₅
Formula weight	831.74
Temperature/K	113.15
Crystal system	monoclinic
Space group	<i>P2₁/c</i>
<i>a</i> /Å	18.5325(6)
<i>b</i> /Å	20.7014(5)
<i>c</i> /Å	12.3772(4)
α/°	90
β/°	109.354(4)
γ/°	90
Volume/Å ³	4480.2(3)
<i>Z</i>	4
ρ _{calc} /cm ³	1.233
μ/mm ⁻¹	0.078
F(000)	1736.0
Crystal size/mm ³	0.27 × 0.22 × 0.18
Radiation	Mo Kα (λ = 0.71073)
2θ range for data collection/°	4.004 to 52.742
Index ranges	-23 ≤ <i>h</i> ≤ 23, -25 ≤ <i>k</i> ≤ 24, -15 ≤ <i>l</i> ≤ 15
Reflections collected	46065
Independent reflections	9116 [R _{int} = 0.0849, R _{sigma} = 0.0661]
Data/restraints/parameters	9116/0/577
Goodness-of-fit on F ²	1.022
Final R indexes [<i>I</i> ≥ 2σ (<i>I</i>)]	R ₁ = 0.0605, wR ₂ = 0.1269
Final R indexes [all data]	R ₁ = 0.0900, wR ₂ = 0.1445
Largest diff. peak/hole / e Å ⁻³	0.21/-0.25

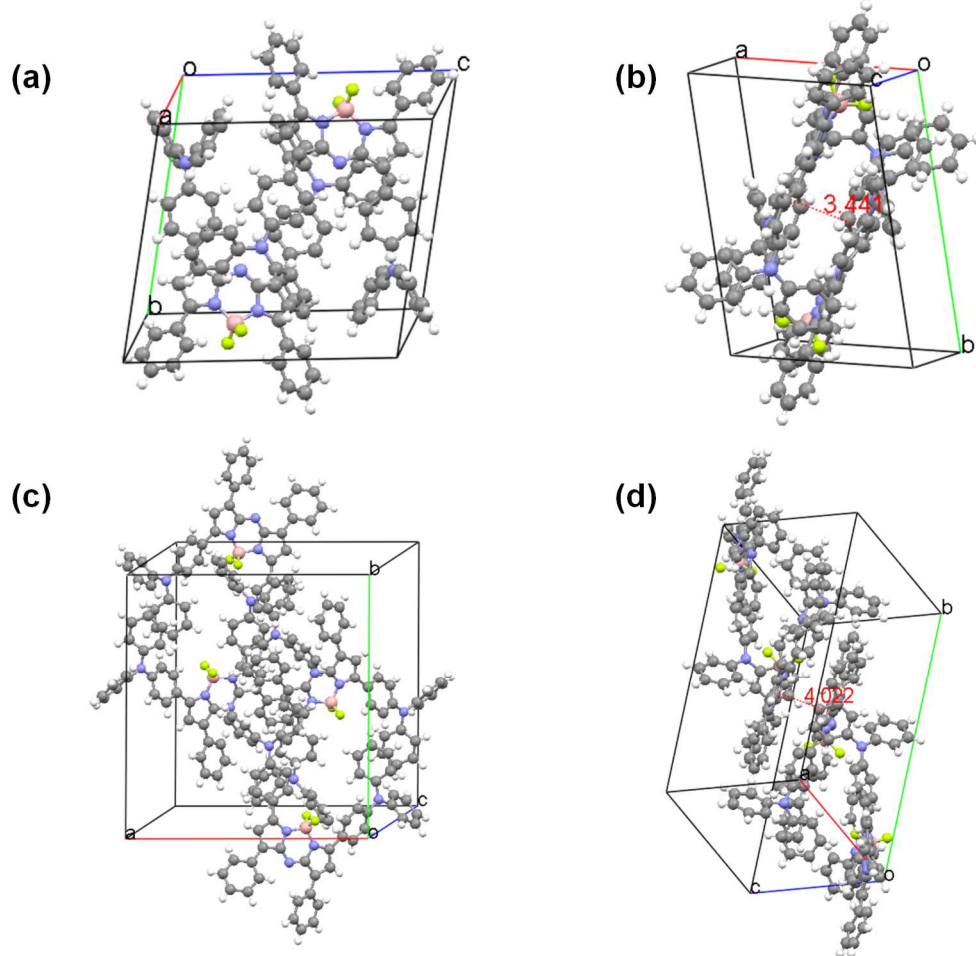


Fig S27. Cell structure diagram of (a) aza-BODIPY 1 and (b) aza-BODIPY 2

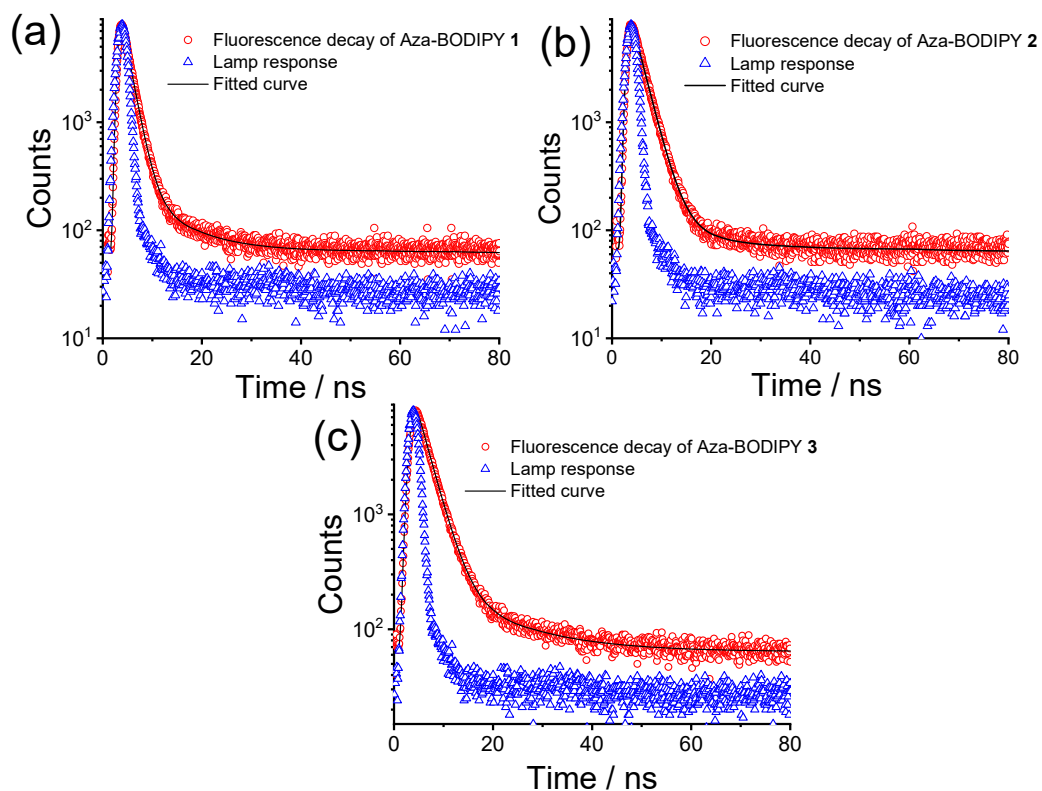


Fig S28. Fluorescence lifetimes decay curve of aza-BODIPY **1-3** in CH₂Cl₂ ($c = 1.0 \times 10^{-6}$ M, $\lambda_{em} = 660, 650, 620$ nm).

Table S3. Fitting parameters for fluorescence lifetimes of dyes **1-3** in CH₂Cl₂. ($c = 1.0 \times 10^{-6}$ M, $\lambda_{em} = 660, 650, 620$ nm).

HTM	$A_1 / \%$	τ_1 / ns	$A_2 / \%$	τ_2 / ns	τ_{ave} / ns
Dye 1	93.31	0.81	6.69	1.8	1.8
Dye 2	76.72	0.93	23.28	2.82	2.8
Dye 3	69.19	1.29	30.81	3.54	3.5

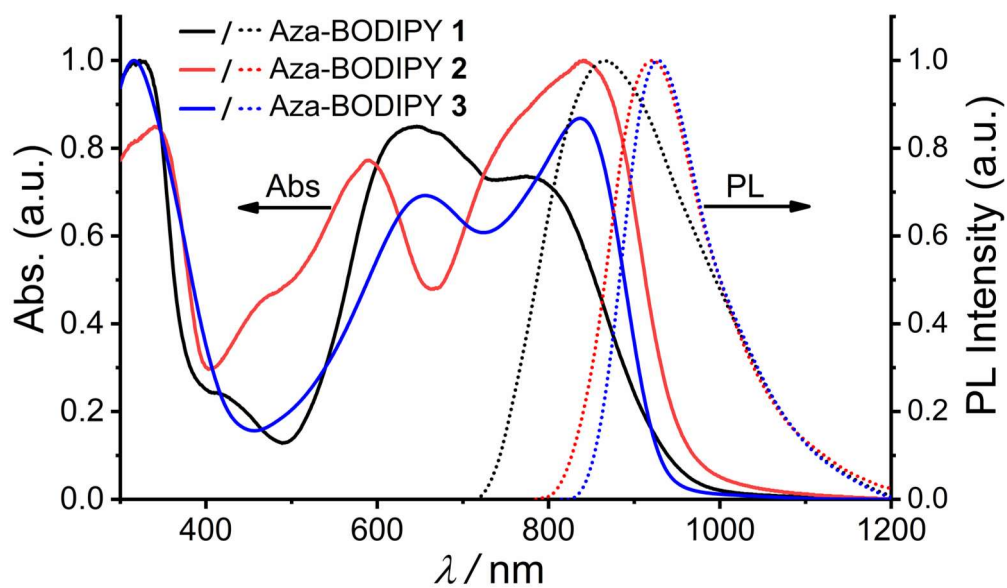


Fig S29. UV/Vis absorption and fluorescence ($\lambda_{\text{ex}} = 700 \text{ nm}$) spectra of the spin-coated thin films of aza-BODIPY 1-3.

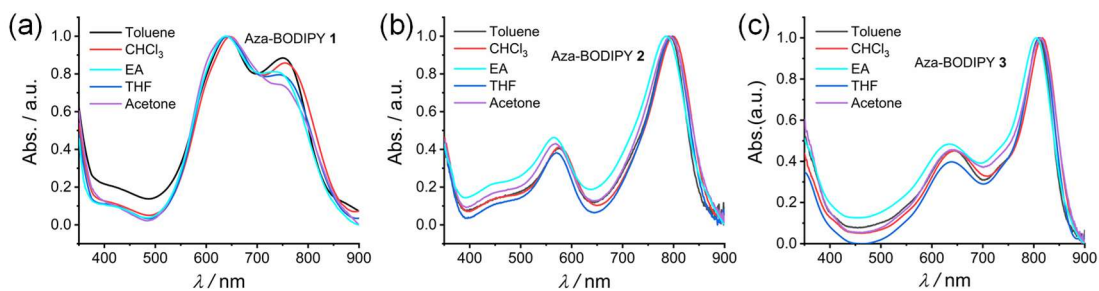


Fig S30. UV/vis spectra of the aza-BODIPY **1-3** in different solvents ($c = 1.0 \times 10^{-6}$ M).

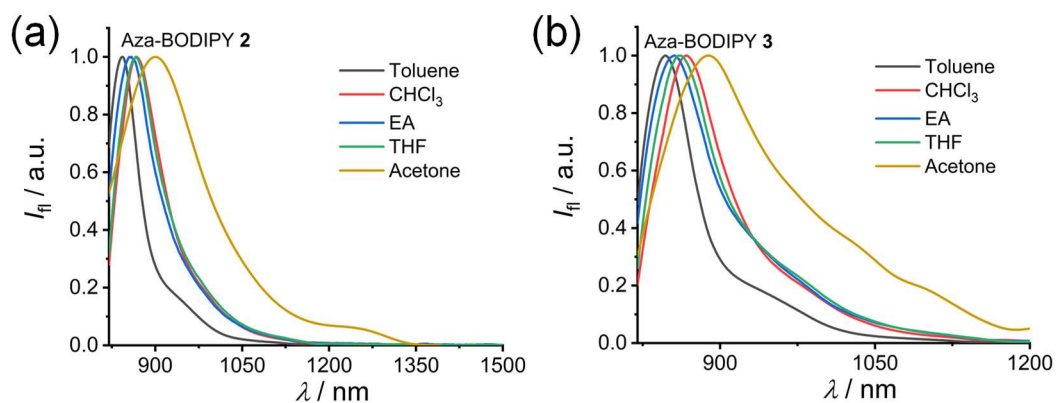


Fig S31. Fluorescence spectra of the aza-BODIPY **2-3** in different solvents ($c = 1.0 \times 10^{-6}$ M, aza-BODIPY **2** and **3**, $\lambda_{\text{ex}} = 800$ nm).

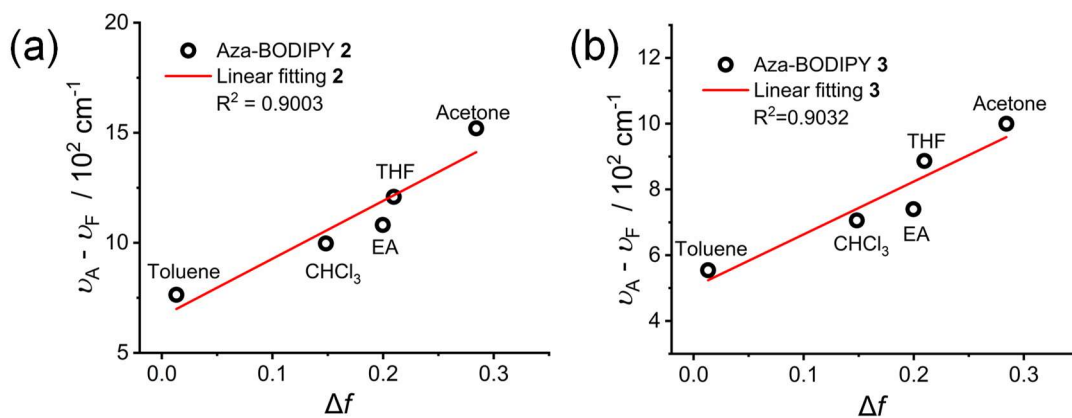


Fig. S32. (a) Lippert–Mataga plots of aza-BODIPY **2**. (b) Lippert–Mataga plots of aza-BODIPY **3**.

Table S4. Spectroscopic data of aza-BODIPY **1** in different solvents.

Solvents	n	ϵ	Δf	λ_A (nm)	λ_F (nm)	$\nu_A-\nu_F$ (cm ⁻¹)
Toluene	1.50	2.379	0.0131	752	848	1505.42
Chloroform	1.45	4.81	0.1483	756	913	2273.74
Ethyl acetate	1.37	6.02	0.1998	740	928	2737.65
Tetrahydrofuran	1.41	7.58	0.2096	750	936	2649.57
Acetone	1.36	20.70	0.2842	750	1015	3481.11

Table S5. Spectroscopic data of aza-BODIPY **2** in different solvents.

Solvents	n	ϵ	Δf	λ_A (nm)	λ_F (nm)	$\nu_A-\nu_F$ (cm ⁻¹)
Toluene	1.4969	2.38	0.0131	792	843	763.87
Chloroform	1.4459	4.81	0.1483	798	867	997.30
Ethyl acetate	1.3723	6.02	0.1998	786	859	1081.20
Tetrahydrofuran	1.407	7.58	0.2096	797	882	1209.18
Acetone	1.359	20.70	0.2842	793	916	1520.31

Table S6. Spectroscopic data of aza-BODIPY **3** in different solvents.

Solvents	n	ϵ	Δf	λ_A (nm)	λ_F (nm)	$\nu_A-\nu_F$ (cm ⁻¹)
Toluene	1.4969	2.38	0.0131	809	847	554.56
Chloroform	1.4459	4.81	0.1483	817	867	705.88
Ethyl acetate	1.3723	6.02	0.1998	805	856	740.12
Tetrahydrofuran	1.407	7.58	0.2096	812	875	886.70
Acetone	1.358	20.70	0.2842	814	886	1000.10

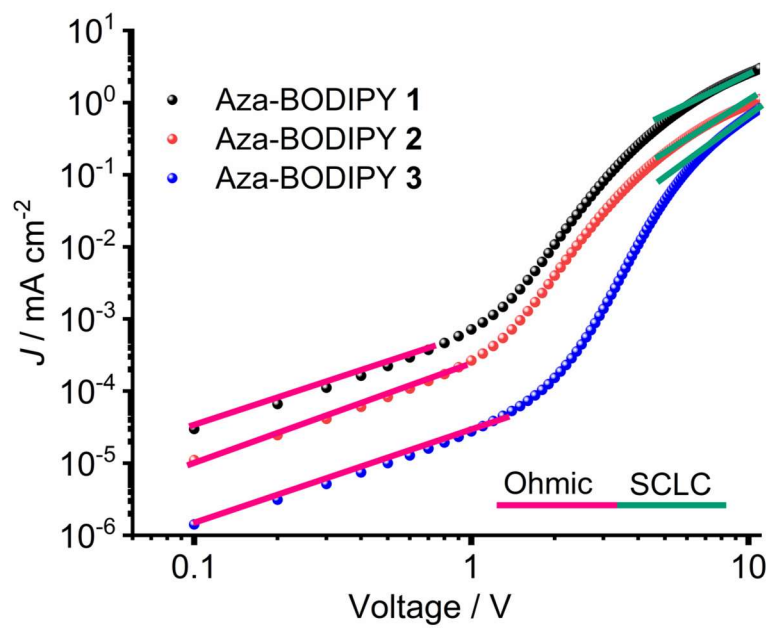


Fig S33. J - V curves based on aza-BODIPY 1-3 single carrier device.

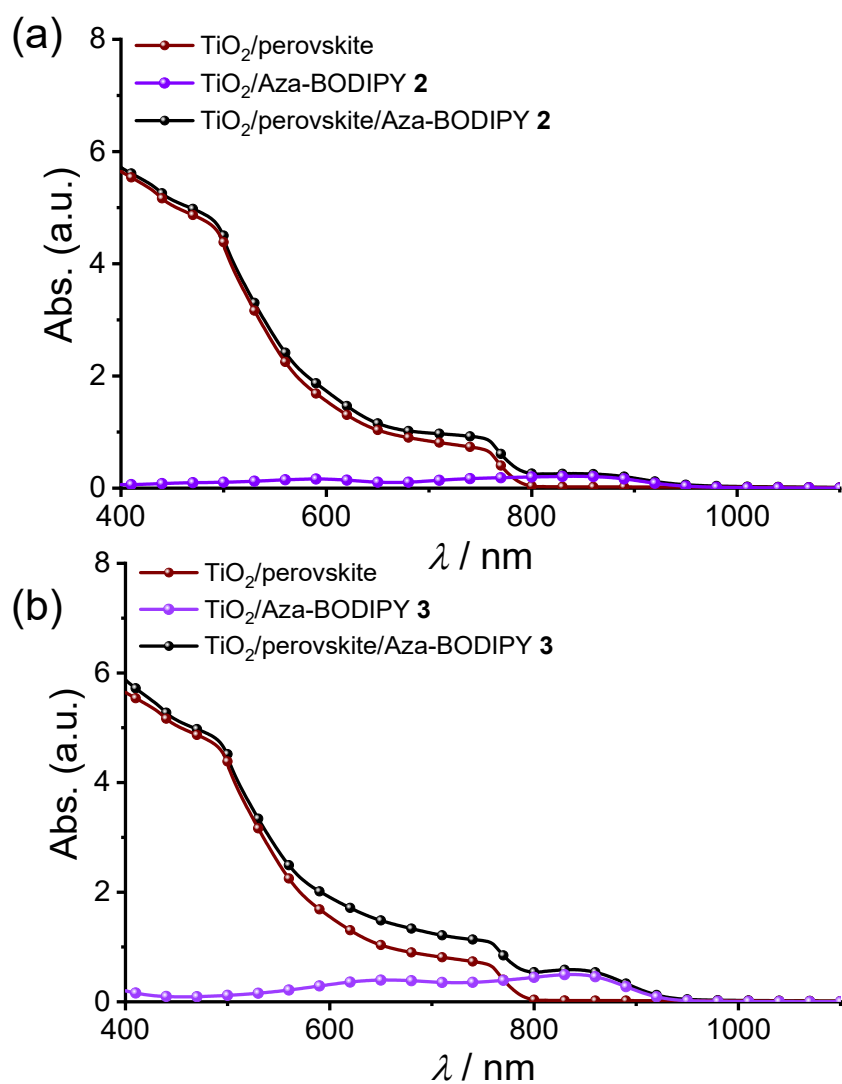


Fig S34. (a) UV/Vis absorption spectra of **2** coated on mesoporous TiO_2 and $\text{TiO}_2/\text{perovskite}$ films, with the spectrum of a $\text{TiO}_2/\text{perovskite}$ film without HTMs shown for comparison. (b) U/Vis absorption spectra of **2** coated on mesoporous TiO_2 and $\text{TiO}_2/\text{perovskite}$ films, with the spectrum of a $\text{TiO}_2/\text{perovskite}$ film without HTMs shown for comparison.

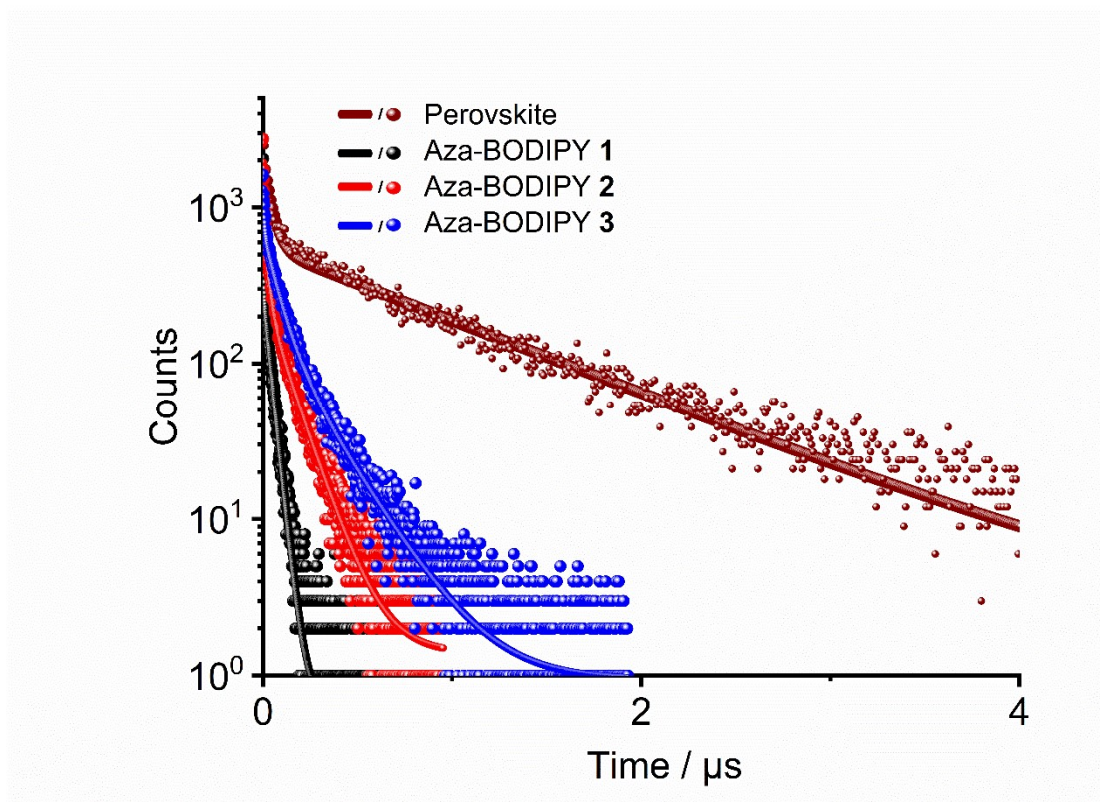


Fig S35. Time-resolved fluorescence spectroscopy of aza-BODIPY **1-3** deposited on perovskite films.

Table S7. Fitting parameters for time-resolved fluorescence spectroscopy of perovskite films based on different HTMs on glass substrate.

HTM/Perovskite	$A_1 / \%$	τ_1 / ns	$A_2 / \%$	τ_2 / ns	$\tau_{\text{ave}} / \text{ns}$
Perovskite	29.7	56.9	70.3	972.6	727.3
Dye 1	96.3	3.0	3.7	161.1	67.3
Dye 2	90.7	10.3	9.3	237.4	185.2
Dye 3	76.1	15.2	23.9	253.1	218.7

3 Perovskite solar cell fabrication and characterization

The preparation of the active layer in the device was based on previous report.⁵ Fluorine-doped tin oxide (FTO) glass was cleaned with deionized water, isopropanol, ethanol, and O₂ plasma. The TiO₂ compact layer (c-TiO₂), mesoporous TiO₂ (m-TiO₂) layer and active layer of perovskite device was fabricated according to our previous reports.^{1,5} The Cs_{0.05}FA_{0.85}MA_{0.10}Pb(I_{0.97}Br_{0.03})₃ perovskite with 5% excess PbI₂ was prepared with PbI₂ (1.60 mmol, 735.3 mg), FAI (1.31 mmol, 224.4 mg), MABr (0.15 mmol, 16.2 mg), and CsI (0.08 mmol, 19.8 mg) in 1 ml mixed solvent of anhydrous dimethylformamide (DMF) and dimethyl sulfoxide (DMSO) (4/1, v/v). The perovskite precursor solution was deposited on the freshly prepared FTO/c-TiO₂/m-TiO₂ substrate, and a two-step spin-coating method was applied. The first step was carried out at 2000 rpm with an acceleration rate of 200 rpm/s for 10 s. The second step followed at 6000 rpm with an acceleration rate of 2000 rpm/s for 30 s. CB (100 μL) was slowly dripped at the 15 s before the second step end. After this, the substrate was annealed at 120 °C for 20 min. In the case of the investigated dopant-free HTMs, all of them were dissolved in chlorobenzene solvent at a concentration of 15 mg mL⁻¹. These HTMs solutions were finally spin coated at 4000 rpm s⁻¹ with an acceleration rate of 2000 rpm/s for 20 s on the perovskite. The substrate was left in a desiccator box for 24 h to oxidize these HTMs. In the end, the gold electrode was thermally evaporated on the surface of aza-BODIPY s. The thickness of the gold electrode was adjusted to 80 nm, and the evaporation speed was adjusted to 0.01 nm s⁻¹ at the first 10 nm, 0.02 nm s⁻¹ for the thickness between 10 nm and 20 nm and 0.08 nm s⁻¹ for the rest 60 nm.

The cross-sectional images of PSCs devices (cross-section and surface) were measured using HitachiSU8010 Scanning Electronic Microscopy (SEM) at accelerating voltage of 10 kV. The PCE, J_{SC} , V_{OC} , FF and $J-V$ curves were obtained by using microenerg's solar cell $I-V$ characteristic measurement system (including a Keithley 2400 digital source meter, a 2000AAA solar simulator, computer and its proprietary Solar Cell Measurement System software), calibrated with a standard silicon cell. All

measurements were performed under ambient conditions, starting at -50 mV and ending at 1250 mV, with 100 sampling points. The data were collected without any modifications for both reverse and forward scans. A metal mask was placed over the devices, exposing only an area of 0.09 cm². Incident photon-to-electron conversion efficiency (IPCE) was measured using E0201a IPCE testing system (Chinese Academy of Science). The measurements were conducted with a scan speed of 10 nm s⁻¹ over an aperture area of 0.09 cm². A monochromatic beam was produced using a CHF-XM-500 W Xenon lamp (AM 1.5 G, 25 °C).

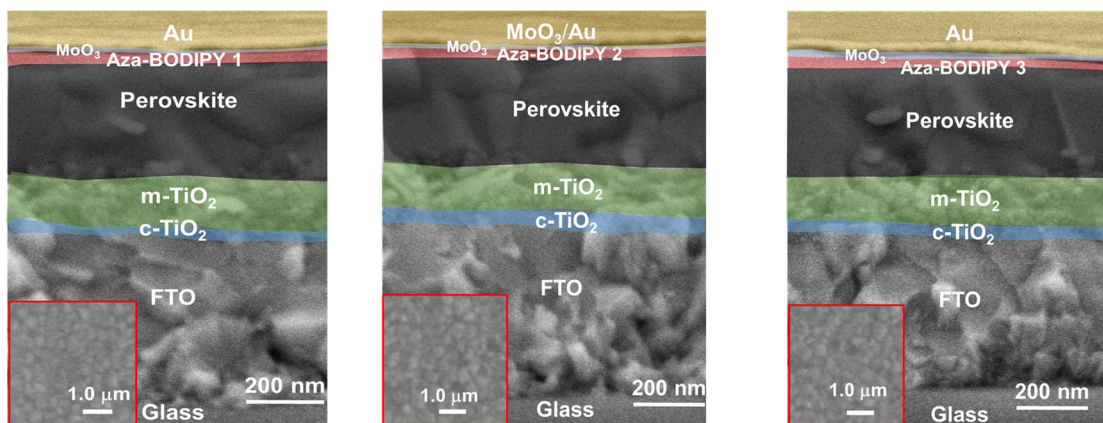


Fig S36. (a) SEM images of different aza-BODIPY **1-3** films on the substrate of FTO/c-TiO₂/m-TiO₂/perovskite (Inset: top-view SEM image of the film of HTM **1-3** on the substrate of FTO/c-TiO₂/m-TiO₂/perovskite).

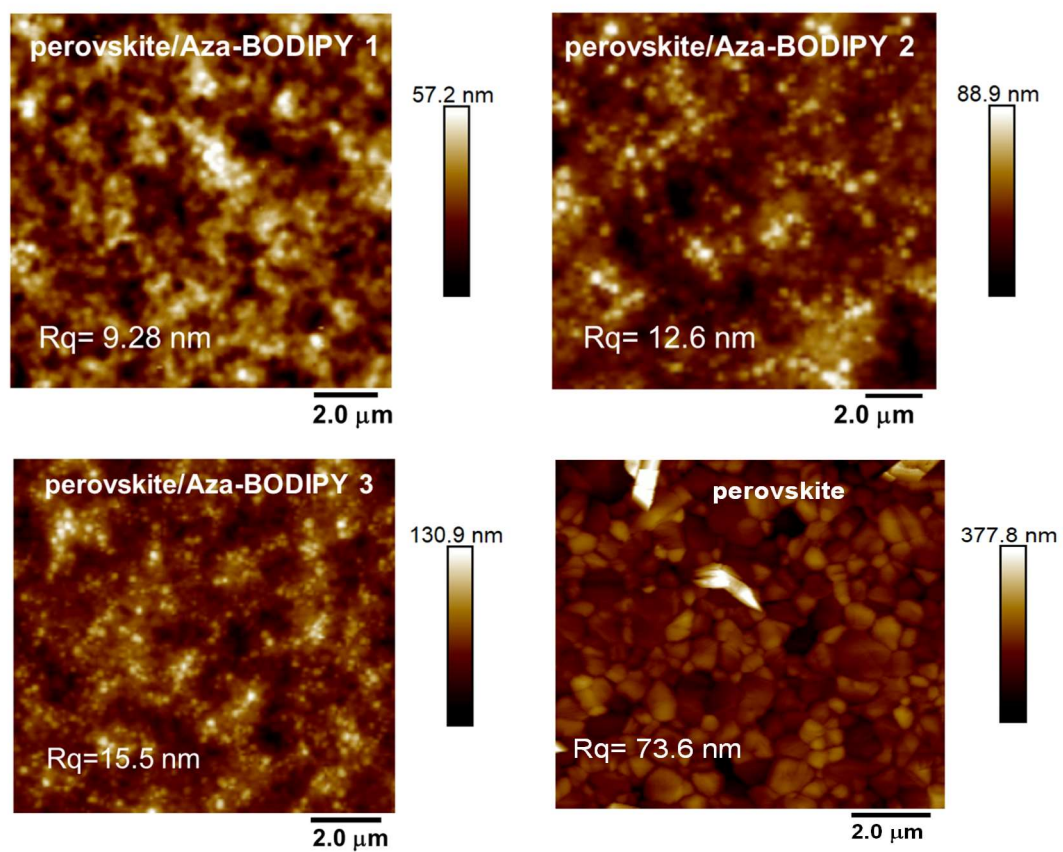
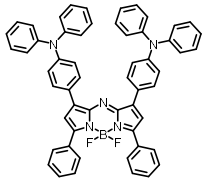
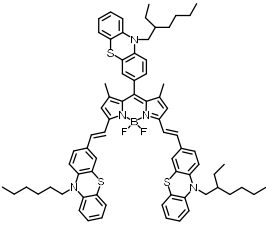
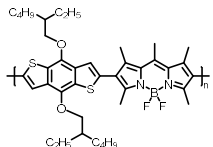
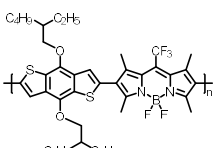
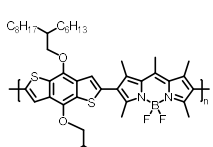
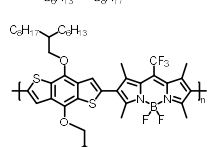
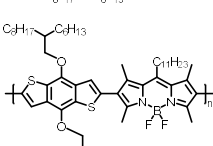
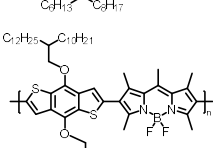
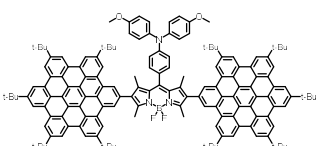
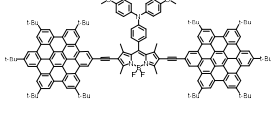
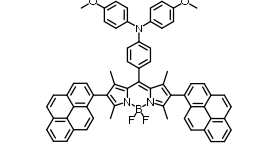
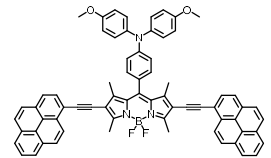
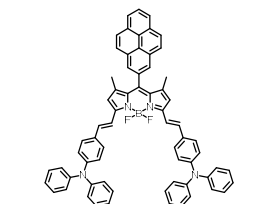
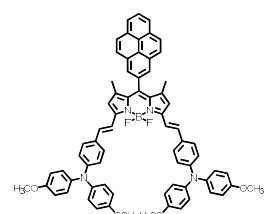
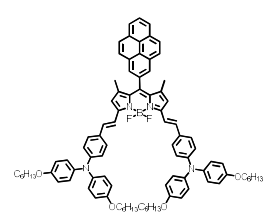
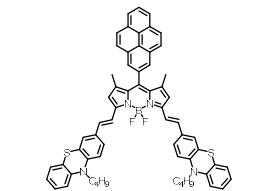
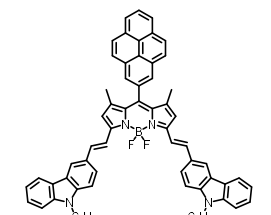


Fig S37. AFM topography of aza-BODIPY 1-3 deposited on perovskite films and pure perovskite films.

Table S8. Summary of HTMs based on (aza-)BODIPY derivatives for PSCs.

Sample	Molecular structure	Device structure	FF /%	PCE /%	Ref. No.
HTM 1 this work		FTO/c-TiO ₂ /m-TiO ₂ / (FAPbI ₃) _{0.875} (MAPbBr ₃) _{0.075} (CsPbI ₃) _{0.05} (PbI ₂) _{0.03} /HTM/Au	74	18.12	this work
PTZ-PTZ-BDP		ITO/SnO ₂ /MAPbI ₃ /HTM/Au	67	14.6	[6]
K1		ITO/HTM/PFN/MAPbI ₃ /PCBM/ZrAcac/Al	78	16.02	[7]
K2		ITO/HTM/PFN/MAPbI ₃ /PCBM/ZrAcac/Al	55	3.85	[7]
K3		ITO/HTM/PFN/MAPbI ₃ /PCBM/ZrAcac/Al	73	12.50	[7]
K4		ITO/HTM/PFN/MAPbI ₃ /PCBM/ZrAcac/Al	62	6.45	[7]
K5		ITO/HTM/PFN/MAPbI ₃ /PCBM/ZrAcac/Al	76	14.65	[7]
K6		ITO/HTM/PFN/MAPbI ₃ /PCBM/ZrAcac/Al	75	13.77	[7]
TM-01		ITO/HTM /Cs _{0.17} FA _{0.83} PbI ₃ /PC ₆₀ BMBP/Ag	75	16.98	[8]

Sample	Molecular structure	Device structure	FF /%	PCE /%	Ref. No.
TM-02		ITO/HTM /Cs _{0.17} FA _{0.83} PbI ₃ / PC ₆₀ BM/BCP/Ag	83	20.26	[8]
TM-03		ITO/HTM /Cs _{0.17} FA _{0.83} PbI ₃ / PC ₆₀ BM/BCP/Ag	76	18.15	[8]
TM-04		ITO/HTM /Cs _{0.17} FA _{0.83} PbI ₃ / PC ₆₀ BM/BCP/Ag	82	19.12	[8]
PyBDP-1		ITO/HTM /Cs _{0.17} FA _{0.83} PbI ₃ / PC ₆₀ BM/BCP/Ag	83	20.37	[9]
PyBDP-2		ITO/HTM /Cs _{0.17} FA _{0.83} PbI ₃ / PC ₆₀ BM/BCP/Ag	83	19.10	[9]
PyBDP-3		ITO/HTM /Cs _{0.17} FA _{0.83} PbI ₃ / PC ₆₀ BM/BCP/Ag	82	19.97	[9]
PyBDP-4		ITO/HTM /Cs _{0.17} FA _{0.83} PbI ₃ / PC ₆₀ BM/BCP/Ag	81	19.05	[9]
PyBDP-5		ITO/HTM /Cs _{0.17} FA _{0.83} PbI ₃ / PC ₆₀ BM/BCP/Ag	75	18.36	[9]

4. References

- [1] H. Bao, H. Liu, S. Wang, J. Ma and X. Li, Restricting lithium-ion migration via Lewis base groups in hole transporting materials for efficient and stable perovskite solar cells, *Chem. Eng. J.*, 2022, **433**. 133534.
- [2] O. V. Dolomanov, L. J. Bourhis, R. J. Gildea, J. A. K. Howard and H. Puschmann, OLEX2: a complete structure solution, refinement and analysis program, *J. Appl. Crystallogr.*, 2009, **42**, 339-341.
- [3] G. M. Sheldrick, *SHELXT* - Integrated space-group and crystal-structure determination, *Dyes, Acta Crystallogr., Sect. A: Found. Adv.*, 2015, **71**, 3-8.
- [4] G. M. Sheldrick, Crystal structure refinement with *SHELXT*, *Acta Crystallogr., Sect. C: Struct. Chem.*, 2015, **71**, 3-8.
- [5] H. Zhu, Z. Shen, L. Pan, J. Han, F. T. Eickemeyer, Y. Ren, X. Li, S. Wang, H. Liu and X. Dong, Low-cost dopant additive-free hole-transporting material for a robust perovskite solar cell with efficiency exceeding 21%, *ACS Energy Lett.*, 2020, **6**, 208-215.
- [6] J. M. Dos Santos, L. K. Jagadamma, M. Cariello, I. D. W. Samuel and G. Cooke, A BODIPY small molecule as hole transporting material for efficient perovskite solar cells, *Sustainable Energy Fuels*, 2022, **6**, 4322-4330.
- [7] M. Kyeong, J. Lee, K. Lee and S. Hong, BODIPY-Based Conjugated Polymers for Use as Dopant-Free Hole Transporting Materials for Durable Perovskite Solar Cells: Selective Tuning of HOMO/LUMO Levels, *ACS Appl Mater Interfaces*, 2018, **10**, 23254-23262.
- [8] J. S. Rocha - Ortiz, J. Wu, J. Wenzel, A. J. Bornschlegl, J. D. Perea, S. Leon, A. Barabash, A. S. Wollny, D. M. Guldi, J. Zhang, A. Insuasty, L. Lüer, A. Ortiz, A. Hirsch and C. J. Brabec, Enhancing Planar Inverted Perovskite Solar Cells with Innovative Dumbbell - Shaped HTMs: A Study of Hexabenzocoronene and Pyrene - BODIPY - Triarylamine Derivatives, *Adv. Funct. Mater.*, 2023, **33**, 2304262.

- [9] I. Seoneray, J. Wu, J. S. Rocha-Ortiz, A. J. Bornschlegl, A. Barabash, Y. Wang, L. Lüer, J. Hauch, A. García, J. Zapata-Rivera, C. J. Brabec and A. Ortiz, Unveiling the Role of BODIPY Dyes as Small-Molecule Hole Transport Material in Inverted Planar Perovskite Solar Cells, *Solar RRL*, 2024, **8**, 2400225.